Numerical Simulation of Liquid-Solid, Solid-Liquid Phase Change Using Finite Element Method in *h,p,k* Framework with Space-Time Variationally Consistent Integral Forms

By

Michael Truex

Submitted to the graduate degree program in Mechanical Engineering

and the Graduate Faculty of the University of Kansas

in partial fulfillment of requirements for the degree of

Master of Science.

Dr. Karan S. Surana, Chairperson

Dr. Albert Romkes

Dr. Peter W. Tenpas

Dr. Bedru Yimer

Date Defended: _____

The Thesis Committee for Michael Truex certifies

that this is the approved version of the following thesis:

Numerical Simulation of Liquid-Solid, Solid-Liquid Phase Change Using Finite Element Method in ***h,p,k*** Framework with Space-Time Variationally Consistent Integral Forms

_____

Dr. Karan S. Surana, Chairperson

_____

Dr. Albert Romkes

_____

Dr. Peter W. Tenpas

_____

Dr. Bedru Yimer

Date Approved:_____

Acknowledgements

I would like to thank Dr. Karan S. Surana, Deane E. Ackers Distguished Professor of Mechanical Engineering, chairman and advisor of my reseach committee. Dr. Surana was the only member of the research faculty who showed interest in me and believed that I belonged in a research role in graduate school. When I started my graduate career, I was a very naive undergraduate student. In just two years, he has transformed me into a confident, competent engineer and I cannot express enough gratitude to him. The knowledge he bestowed upon me led to the work that is included in this thesis. I would also like to thank Dr. Albert Romkes, Dr. Peter Tenpas, and Dr. Bedru Yimer for serving on the committee for my thesis defense.

Most of all, this thesis is dedicated to my parents, Robert and Mary Ann Truex. Without their unwavering support and constant encouragement, I would have never attended graduate school and produced the work contained in this thesis.

Abstract

This thesis presents development of mathematical models for liquid-solid phase change phenomena using Lagrangian description with continuous and differentiable smooth interface (transition region) between the solid and the liquid phases in which specific heat, thermal conductivity, and latent heat of fusion are a function of temperature. The width of the interface region can be as small or as large as desired in specific applications. The mathematical models presented in the thesis assume homogeneous and isotropic medium, zero velocity field (no flow) with free boundaries i.e. stress free domain. With these assumptions the mathematical model reduces to the first law of thermodynamics i.e. energy equation. The mathematical models presented here are neither labeled as enthalpy models or others, instead these are based on a simple statement of the first law of thermodynamics using specific total energy and heat vector augmented by the constitutive equation for heat vector i.e. Fourier heat conduction law and the statement of total specific energy incorporating the physics of phase change in the smooth interface region between solid and liquid phases. This results in a time dependent non-linear convection diffusion in temperature in which physics of interface initiation and propagation is intrinsic and thus avoids front tracking methods. This can also be cast as a system of first order PDEs using auxiliary variables and auxiliary equations if so desired due to the use of specific methods of approximation as done in the present work.

The numerical solutions of the initial value problems resulting from the mathematical models are obtained using space-time least squares finite element process based on minimization of the residual functional. This results in space-time variationally consistent integral forms that yield symmetric algebraic systems with positive definite coefficient

matrices that ensure unconditionally stable computations during the entire evolution. The local approximations for the space-time finite elements are considered in ***h,p,k*** framework which permits higher degree as well as higher order local approximations in space and time. Computations of the evolution are performed using a space-time strip or slab corresponding to an increment of time with time marching procedure. 1D numerical studies are presented and the results are compared with sharp interface and phase field methods. Numerical studies also presented for 1D and 2D model problems in which initiation as well as propagation of the interface is demonstrated. These studies cannot be performed using sharp interface and phase field models.

The significant aspects of the present work are: (i) the smooth interface permits desired physics and avoids singular fronts that are non physical (ii) the mathematical model resulting from the present approach is a non-linear diffusion equation, hence intrinsically containing the ability to initiate as well as locate the front during evolution and hence no special front tracking methods are needed. (iii) This methodology permits initiation of the interface i.e. it permits initiation of the phase change phenomena. This is not possible in sharp interface and phase field methods. (iv) The computational infrastructure used ensures stable computations and high accuracy of evolution for each time step and hence time accurate evolutions are possible.

Contents

List of Tables

List of Figures

Nomenclature

ρ	Density
c	Specific Heat
c_p	Specific Heat
c_s	Specific Heat in Solid Phase
c_{ps}	Specific Heat in Solid Phase
c_l	Specific Heat in Liquid Phase
c_{pl}	Specific Heat in Liquid Phase
k	Thermal Conductivity
k_s	Thermal Conductivity in Solid Phase
k_l	Thermal Conductivity in Liquid Phase
L	Latent Heat of Fusion
L_f	Latent Heat of Fusion
T	Temperature
T_s	Temperature in Solid Phase
T_l	Temperature in Liquid Phase
T_{sat}	Saturation Temperature
u	Temperature
u_f	Fusion Temperature

$\boldsymbol{n}$	Unit Exterior Normal
v_n	Normal Velocity of Sharp Interface
Γ	Liquid-Solid Interface Boundary
Ω	Domain
Ω_x^s	Domain of Solid
Ω_x^l	Domain of Liquid
h	Enthalpy
h_s	Specific Enthalpy
S	Source Term
f	Liquid Fraction
p	Phase Field Variable
F	Free Energy Functional
ξ	Parameter that Controls Interface Length in Phase Field
α	Relaxation Time
$\boldsymbol{q}$	Fourier Heat Conduction
q_x	Heat Conduction in x-direction
q_y	Heat Conduction in y-direction
e	Specific Total Energy
$\boldsymbol{\nabla}$	Del (Gradient) Operator
$\boldsymbol{\phi}$	Vector of Dependent Variables
$\boldsymbol{\phi}_h$	Global Approximation of $\boldsymbol{\phi}$
$\boldsymbol{\phi}_h^e$	Local Approximation of $\boldsymbol{\phi}$
n_e	Number of Equations

p-level	Degree of Local Approximation
E_i^e	Error (Residual) Equation for an Element 'e'
V_h	Approximation Space
$I(\boldsymbol{\phi}_h)$	Error Functional in Least Squares Finite Element Formulation
$\boldsymbol{g}$	Measure of how well GDE is Satisfied in Point-Wise Sense
PDEs	Partial Differential Equations
IVPS	Initial Value Problems
AHC	Apparent Heat Capacity Method
LINH	Linearization Method
GM	Galerkin Method
STGM	Space-time Galerkin Method
PGM	Petrov Galerkin Method
STPGM	Space-time Petrov Galerkin Method
WRM	Weighted Residuals Method
STWRM	Space-time Weighted Residuals Method
GM/WF	Galerkin Method with Weak Form
STGM/WF	Space-time Galerkin Method with Weak Form
STVC	Space-time Variational Consistent
STVIC	Space-time Variational Inconsistent
LSFEF	Least Squares Finite Element Formulation
STLSP	Space-time Least Squares Process

Chapter 1

Introduction

Numerical simulation of phase change phenomena has been a subject of research for over a century. There are three main sources of difficulties in the numerical simulation of phase change phenomena. First, the mathematical models are a system of non-linear partial differential equations (PDEs) in space coordinates and time, hence they are initial value problems (IVPs) describing the evolution. Secondly, the idealized physics of phase change phenomena creates sharp moving fronts, their precise locations and movement being of interest. Thirdly, the first two aspects of the phase change phenomena require selection of prudent, robust, unconditionally stable and time accurate computational methods for obtaining numerical solutions i.e. evolutions of the associated IVPs. Due to the insistence on the use of finite difference methods, finite volume methods, and more recently finite element methods based on Galerkin method with weak form (GM/WF) that lack the desired features necessary to address numerical simulations of such initial value problems in an accurate and reliable manner many issues remain unresolved. This has resulted in computational methodologies that are less than satisfactory. In this brief introduction we

present various approaches for deriving mathematical models based on the assumptions related to the physics of phase change phenomena that are commonly used in the published work and discuss their merits and shortcomings. This is followed by a brief discussion of the computational methods currently employed in conjunction with various mathematical models. The last section contains the scope of present work and discussion of the methodologies employed in the development of the mathematical models and the computational infrastructure employed for obtaining numerical solutions of the associated IVPs.

1.1 Mathematical Models

First, we consider the mathematical models that are currently used for phase change phenomena. These essentially fall into three categories: Sharp interface models, enthalpy models, and phase field models. The sharp interface models assume that the liquid and solid phases are separated by a sharp interface (hypothetically, an infinitely thin curve or surface). The latent heat of fusion is supposed to be instantaneously released or absorbed along the interface. This of course results in a step change along the interface, hence the name sharp interface model. In this approach, we have individual mathematical models for liquid and solid phases. At the interface, energy balance provides conditions that determine the movement of the interface. The sharp interface models are also called Stefan models and were derived by J. Stefan [1] who studied the freezing of ground. The mathematical details of the sharp interface model are presented in Chapter 2. When the mathematical model for sharp interface is posed as a system of integral equations, proof of existence and uniqueness of the classical solution was provided by Rubenstein in 1947 [2]. For the one dimensional case, an analytical solution was derived in reference [3] for the temperature

distribution (also presented in Chapter 2). We remark that sharp interface models obviously require sharp front tracking.

The second class of mathematical models fall into the category of enthalpy methods. In these methods the energy equation is cast in terms of enthalpy and temperature. This is augmented by the enthalpy equation. The motivation for these methods is to avoid front tracking and rely on computations on a fixed grid. The main merit of this method is that it eliminates the heat flux balance at the interface. The formulation of the mathematical models in this approach can be done in many different ways [4, 5], details of some models presented in Chapter 2. These methods generally introduce a mushy zone (narrow) between the liquid and solid phases, eliminating the singular nature of the front inherent in sharp interface models. The concept of liquid fraction is introduced in the mushy zone to account for the fact that this zone may contain a mixture of liquid and solid. There appears to be increasing emphasis in the published work on numerical methods (rather than mathematical models) for phase change problems [6]. The commonly used methods are referred to as source update methods, linearization method (LINH), and apparent heat capacity method (AHC). Our view on this issue is drastically different. If we note that the space-time differential operators in phase change models are either non-self adjoint or non-linear, we must seek a computational infrastructure that addresses numerical solution of IVPs containing these operators in an unconditionally stable and time accurate manner. This in fact is the methodology employed in the present work. We note that in the enthalpy models, the sharp interface models requiring tracking of a sharp moving front is converted into a non-linear diffusion problem, the main benefit of these models.

The third category of mathematical models for phase change phenomena are called phase field models. These models are based on the pioneering work of Cahn and Hilliard

[7]. In this approach, the sharp interface is replaced by a smooth interface or smooth transition region between the liquid and solid phases. The mathematical models in the phase field method are derived using Landau-Ginzburg [8] theory of phase transition. The method in short can be summarized as being founded on standard mean theories of critical phenomena based on a free energy functional. Hence the method obviously relies on specification of free energy density function, which is the main driving force for phase transition. This method has shown good agreement with the 1D Stephan problem. Details of the mathematical model (for 1D case) for phase field method are also presented in Chapter 2. While the phase field method eliminates the necessity of computations with sharp interfaces and tracking of fronts, the main disadvantages of this approach are: (i) It requires a priori knowledge of the free energy density function for the application under consideration. (ii) The mathematical model in these approaches are unable to simulate the initiation of liquid-solid interface, hence the liquid-solid or solid-liquid phases with known interface location must be defined as initial condition. This limitation is due to the specific nature of the free energy density function (generally a double well potential, see Chapter 2). However, if a liquid-solid interface is specified as initial conditions, then the phase field mathematical models are quite effective in simulating its movement during evolution. In most (if not all) engineering applications the detection of the initial formation of the solid-liquid interface is essential as it may not be possible to know its location a priori. These two limitations have resulted in lack of widespread use of these models in phase change phenomena in practical applications.

1.2 Computational Methodology

We note that the mathematical models for the phase change phenomena are generally non-linear PDEs in space coordinates and time and hence they result in non-linear IVPs. With realistic physics, the mathematical models are complex enough not to permit determination of theoretical solutions, hence numerical solutions of IVPs are essential. Broadly speaking, the computational methods for IVPs can be classified in two groups [9–12]: space-time decoupled methods and space-time coupled methods. In the space-time decoupled methods, for an instant of time, the time derivatives are assumed constant and spatial discretization is performed. This reduces the PDEs in space and time to ODEs in time which are then integrated using explicit or implicit integration methods and other techniques to obtain the evolution. Almost all of the finite difference, finite volume, and finite element methods (GM/WF) used currently [10] for IVPs fall into the space-time decoupled category. The assumption of constant time derivative necessitates extremely small time increments during the integration of ODEs in time. The issues of stability, accuracy, and lack of time accurate evolutions are well known. Currently used numerical methods for phase change problems fall into this category. The non-current treatment in space and time is contrary to the physics in which all dependent variables exhibit simultaneous dependence on space coordinates and time. That is, as time elapses the values of the dependent variables at the material points in the spatial domain change. Another significant point to note is that in a large majority of published work on phase change problems, often the distinction between mathematical model and computational methods or approaches is not clear. As a consequence, it is difficult to determine if the non-satisfactory numerical solutions are a consequence of the numerical methods used or deficiencies in the mathematical models.

The space-time coupled methods on the other hand maintain simultaneous dependence of the dependent variables on space coordinates and time [9, 11, 12]. In these methods, the discretizations in space and time are concurrent and hence in agreement with the physics of evolution described by the IVPs. These methods are far more superior than the space-time decoupled methods in terms of mathematical rigiour as well as accuracy. Whether to choose space-time finite difference, finite volume, or finite element method depends upon the mathematical nature of the space-time differential operator and whether the computational strategy under consideration will yield unconditionally stable computations, will permit error assessment, and will yield time accurate evolution upon convergence (see Chapter 3).

1.3 Scope of Work

In the present work we consider simple 1D and 2D phase change problems in which the mathematical models are in Lagrangian description using the assumption of no flow and absence of stress field. Thus the mathematical model only consists of the energy equation. Secondly, for the physics of phase change to be incorporated in the mathematical model we need a clear description of the physics of phase change we wish to consider. We assume that the phase change phenomena is associated with a transition zone (say from liquid to solid) in which the specific heat and thermal conductivity change from values that are associated with one phase to the values associated with the other phase in a continuous and differentiable manner over a small temperature range. The latent heat of fusion is assumed to behave in a similar fashion. This assumption of transition zone is reasonable and valid even for the purest materials (observed experimentally). With the transition region defining

the specific heat, conductivity, and the latent heat of fusion in a continuous and differentiable manner, we eliminate the sharp interface and instead we have a smooth interface. Secondly, the problem of tracking a sharp moving interface now reduces to a non-linear diffusion equation. We remark that the choice of dependent variables, say temperature or enthalpy as argued in literature, is irrelevant in the present work. The smoothness of the solution of the IVP is a consequence of the smoothness of the phase change phenomenon incorporated in the mathematical model. Thus the proposed method is not an enthalpy method, but rather a smooth interface method. The mathematical model is derived as usual using specific total energy and heat vector (due to the assumption of no flow and absence of stress field). The specific total energy is expressed in terms of storage and latent heat of fusion. By substituting the specific total energy in the energy equation, we obtain a single PDE in temperature (assuming Fourier heat conduction law) and latent heat of fusion that contains up to second order derivatives of temperature in the spatial coordinates but only first order derivatives of the temperature and the latent heat with respect to time. The description of latent heat over the spatial domain as a function of temperature provides closure to the mathematical model. The details of the mathematical model for 1D and 2D phase change phenomena are presented in Chapter 2. This mathematical model is a non-linear diffusion equation in temperature as opposed to enthalpy as argued in the published work to be necessary [4–6] for the computations to function properly.

Since the mathematical models are non-linear PDEs in space and time, i.e. non-linear IVPs, the most suitable strategy for obtaining their numerical solutions [9, 11, 12] is to employ space-time coupled finite element methods. In this case, the space-time differential operator is non-linear, hence space-time Galerkin Method (STGM), space-time Petrov-Galerkin Method (STPGM), space-time Weighted Redsiduals Method (STWRM), and space-

time Galerkin Method with Weak Form (STGM/WF) are all ruled out as viable methodologies for constructing a space-time integral form as these methods yield space-time integral forms that are space-time variationally inconsistent (STVIC) [12]. The STVIC integral forms yield computational processes in which the computations are not always ensured to be unconditionally stable. The space-time least squares process (STLSP) as presented in references [11, 12] yield integral forms that are space-time variationally consistent (STVC) and hence are used in the present. The local approximations are considered in higher order approximation spaces, i.e. ***h,p,k*** spaces or framework [12–15]. This permits desired global differentiability approximation in space and time. The STLSP and the details specific to the mathematical models and approximation spaces used in the present work are described in Chapter 3.

Numerical studies for 1D and 2D phase change problems are presented in Chapter 4. The results obtained from the proposed methodology are also compared with those obtained using sharp interface model and phase field model (also computed using STLSP). Summary and conclusions are presented in Chapter 5.

Chapter 2

Mathematical Models

2.1 Introduction

In this chapter we present mathematical models based on sharp interface, enthalpy, and phase field methodologies for phase change phenomena that are commonly used in the published work. These are followed by the details of the mathematical models used in the present work. All these mathematical models are based on the following assumptions:

(1) The mathematical models use Lagrangian description i.e. the position coordinates of the material points in the reference configuration (fixed) and time are independent variables.

(2) We assume that the velocity field is identically zero i.e. no flow assumption.

(3) The spatial domain is assumed to be free of stress field i.e. the IVPs describing phase change are posed as free boundary problems.

(4) Based on assumptions (2) and (3), continuity and momentum equations are identi-

cally satisfied and hence need not be considered as part of the mathematical models.

(5) Hence we only need to consider energy equation in which viscous effects are absent due to assumption (2).

Thus, the mathematical models under these assumptions consist of energy equation supplemented by the physics of phase change that varies depending upon the choice of modeling approach (sharp interface, enthalpy, phase field, or smooth interface). For simplicity we only present details of the published mathematical models that are commonly used for 1D case.

2.2 Sharp Interface Models

Under the assumption stated here, the mathematical model in this approach reduces to heat conduction in isotropic medium for each of the two phases supplemented by the heat balance statement at the interface separating the two phases. The interface is assumed to be infinitely thin. Furthermore, these mathematical models assume constant (and same) specific heat c_p and thermal conductivity k in both liquid and solid phases,

Solid Phase:

$$\rho c_p \frac{\partial T}{\partial t} - \boldsymbol{\nabla} \cdot (k \boldsymbol{\nabla} T_s) = 0 \qquad \forall \, (\boldsymbol{x}, t) \; \in \; \Omega^s_{xt} = \Omega^s_x \times \Omega_t = \Omega^s_x \times (0, \tau) \tag{2.1}$$

Liquid Phase:

$$\rho c_p \frac{\partial T}{\partial t} - \boldsymbol{\nabla} \cdot (k \boldsymbol{\nabla} T_l) = 0 \qquad \forall \, (\boldsymbol{x}, t) \; \in \; \Omega^l_{xt} = \Omega^l_x \times \Omega_t = \Omega^l_x \times (0, \tau) \tag{2.2}$$

At the interface:

$$L_f v_n = [(-k \boldsymbol{\nabla} T_s) - (-k \boldsymbol{\nabla} T_l)] \cdot \boldsymbol{n} \qquad \forall \, (\boldsymbol{x}, t) \; \in \; \Gamma_{x,t} = \Gamma_x \times \Omega_t \tag{2.3}$$

in which Ω_x^s and Ω_x^l are solid and liquid spatial domains, $\Gamma_x(t) = \Omega_x^s \bigcap \Omega_x^l$ is the interface between the two phases, L_f is the latent heat of fusion, $\boldsymbol{n}$ is the unit exterior normal from the solid phase at the interface, and v_n is the normal velocity of the interface. Subscripts s and l signify solid and liquid phases.

When the mathematical model is posed as a system of integral equations, a complete proof of existence and uniqueness of the classical solution in one dimension was provided by Rubenstein in 1947 [2]. For the one dimensional case, an analytical solution was derived in reference [3] for the temperature distribution T.

$$T(x,t) = C_1 \frac{\text{erf}\left(\frac{\beta}{2}\right) - \text{erf}\left(\frac{x}{2\sqrt{t+t_0}}\right)}{\text{erf}\left(\frac{\beta}{2}\right)} \quad ; \quad x \leq \Gamma(t) \tag{2.4}$$

$$T(x,t) = C_2 \frac{\text{erf}\left(\frac{\beta}{2}\right) - \text{erf}\left(\frac{x}{2\sqrt{t+t_0}}\right)}{1 - \text{erf}\left(\frac{\beta}{2}\right)} \quad ; \quad x > \Gamma(t) \tag{2.5}$$

where $C_1 = -0.085$, $C_2 = -0.015$ and the location of the interface, $\Gamma(\tau)$, is defined by,

$$\Gamma(t) = \beta\sqrt{t+t_0} \tag{2.6}$$

where $t_0 = 0.1246$. $\beta = 0.396618$ can be obtained by solving the following equation.

$$\frac{2}{\sqrt{\pi}}\, e^{\beta^2/4} \left[\frac{C_2}{1 - \text{erf}\left(\frac{\beta}{2}\right)} - \frac{C_1}{\text{erf}\left(\frac{\beta}{2}\right)} \right] - \beta = 0 \tag{2.7}$$

In this mathematical model the enthalpy increases or reduces by a large amount during phase change at a constant temperature. This of course poses serious problems in the numerical simulations of the IVPs described by these models.

2.3 Enthalpy Models

We represent some representative mathematical models used in this approach. The first model is due to references [4, 5]. In this model we have,

$$\frac{\partial}{\partial t}(\rho h) - \frac{\partial}{\partial x}\left(k\frac{\partial T}{\partial x}\right) = S \qquad \forall\ (x,t)\ \in\ \Omega_{xt} = \Omega_x \times \Omega_t \tag{2.8}$$

$$h = h_s + fL + c(T - T_{sat}) \tag{2.9}$$

$$f = \begin{cases} 0 & ; \quad h < h_s \\ \dfrac{h - h_s}{L_f} & ; \quad h_s \leq h \leq h_s + L \\ 1 & ; \quad h > h_s + L \end{cases} \tag{2.10}$$

Substituting equation (2.9) into equation (2.8), the governing equation for the enthalpy based model is obtained,

$$\frac{\partial}{\partial t}(\rho c T) + \frac{\partial H}{\partial t} - \frac{\partial}{\partial x}\left(k\frac{\partial T}{\partial x}\right) = S \qquad \forall\ (x,t)\ \in\ \Omega_{xt} = \Omega_x \times \Omega_t \tag{2.11}$$

$$H = \rho\,(h_s + fL - cT_{sat}) \tag{2.12}$$

where h_s is the saturated enthalpy of solid, T_{sat} is the saturated temperature, L is the latent heat, c the specific heat, S is a source term and f is the liquid fraction that accounts for the latent heat capacity present.

Another mathematical model is due to reference [16],

$$\frac{\partial h}{\partial t} - \frac{\partial}{\partial x}\left(k(u)\frac{\partial u}{\partial x}\right) = \quad \forall\ (x,t)\ \in\ \Omega_{xt} = \Omega_x \times \Omega_t \tag{2.13}$$

$$u = \begin{cases} \dfrac{h}{\rho c_s} & ; \quad h < \rho c_s u_f \\ u_f & ; \quad \rho c_s u_f \leq h < \rho\,(c_s u_f + L) \\ u_f + \left(h - \dfrac{\rho\,(c_s u_f + L)}{\rho c_l}\right) & ; \quad h \geq \rho\,(c_s u_f + L) \end{cases} \tag{2.14}$$

where u is the temperature, $h(u)$ is the enthalpy, $k(u)$ is the thermal conductivity, c_s is the specific heat in the solid phase, c_l is the specific heat in the liquid phase, u_f is the fusion temperature, and L is the latent heat of fusion. $k(u)$ is also defined by constant values k_s and k_l in the solid and liquid phases.

These current enthalpy methods lack comparison to sharp interface solutions in the currently published works. Generally, these models have expanded mushy regions that do not have qualitative agreement with phase field approximations and sharp interface solutions.

2.4 Phase Field Models

Let p be the phase field variable. For a pure material, p is assigned a value of -1 in the solid region and $+1$ in the liquid region. The length of the transition zone between solid and liquid regions is controlled by ξ (Figure 2.1).

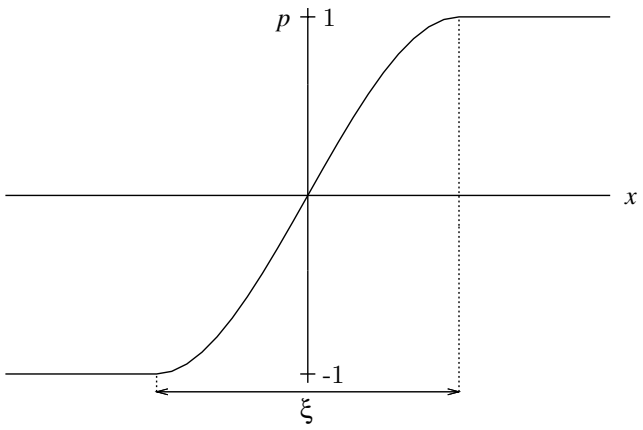

Figure 2.1: Phase transition proportional to ξ

The phase field method was derived using the Landau-Ginzburg theory of phase tran-

sitions [8]. This method relies on standard mean theories of critical phenomena where the free energy functional is defined by,

$$F(p,T) = \int \left(\frac{1}{2}\xi^2 (\nabla p)^2 + f(p,T) \right) dp \tag{2.15}$$

where ξ is a parameter that controls the interface thickness, and $f(p,T)$ is the free energy density of the system that often takes the form of a double well potential, an example of which is shown in Figure 2.2.

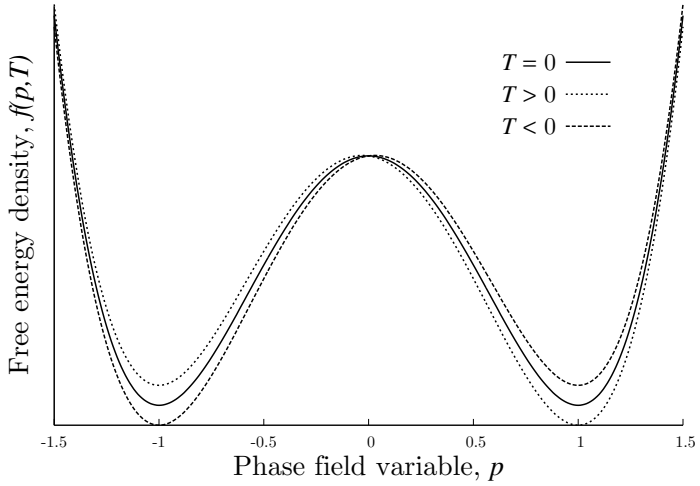

Figure 2.2: Free Energy Density of a Pure Material

The phase field model for a pure material is,

$$\rho c_p \frac{\partial T}{\partial t} - \nabla \cdot (k \nabla T) + \frac{1}{2} L_f \frac{\partial p}{\partial t} = 0 \qquad \forall \ (x,t) \ \in \ \Omega_{xt} = \Omega_x \times \Omega_t = (0,1) \times (0,\tau) \tag{2.16}$$

$$\alpha \xi^2 \frac{\partial p}{\partial t} - \xi^2 \Delta p + \frac{\partial f}{\partial p} = 0 \qquad \forall \ (x,t) \ \in \ \Omega_{xt} = \Omega_x \times \Omega_t = (0,1) \times (0,\tau) \tag{2.17}$$

This model relies on the free energy density, in many cases defined as a polynomial, that is the driving force for the phase transition. For simulations where an interface has been

defined, this model poses no problems and is able to track the moving front accurately. However, when the domain is completely liquid or solid, the free energy density functions currently used do not allow for initiation of a front due to the presence of two distinct minima regardless of the temperature. For example, if a completely liquid domain is considered and heat is removed from one of the boundaries, the phase will remain in a liquid state although the temperature will fall below the freezing temperature. This characteristic poses problems when simulating real engineering applications.

2.5 Mathematical Models used in the Present Work

The mathematical models used in the present work are derived based on the assumption of a smooth interface between the solid and liquid phases over a small temperature range in which specific heat, conductivity, and the latent heat of fusion changes in a continuous and differentiable manner. Figure 2.3 (a-c) shows variations of c_p, k, and L_f in the smooth interface zone between solid and liquid phases defined by the temperatures T_s and T_l.

The range $[T_s, T_l]$ can be as narrow or wide as desired by the physics of phase change in a specific application. The mathematical models presented in the following are neither labeled as enthalpy models nor others, instead these are based on a simple statement of the first law of thermodynamics using specific total energy and heat vector augmented by the constitutive equation for heat vector (Fourier heat conduction law) and the statement of specific total energy incorporating the physics of phase change in the smooth interface zone between the solid and liquid phases. We present the mathematical models for 1D and 2D cases in the following.

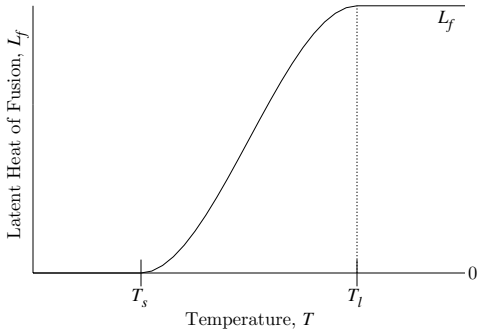

(a) Variation of latent heat in the smooth interface zone

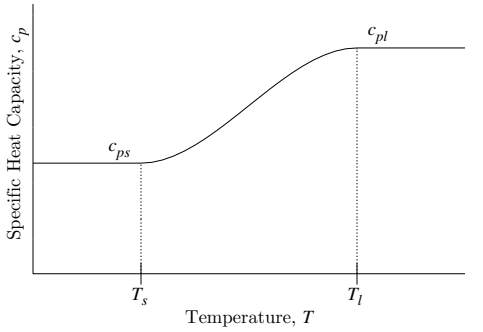

(b) Variation of specific heat in the smooth interface zone

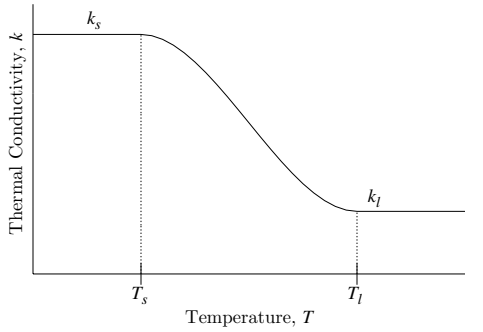

(c) Variation of thermal conductivity in the smooth interface zone

Figure 2.3: Variations of L_f, c_p, and k in the smooth interface zone between the solid and liquid phases

2.5.1 Mathematical Models for 1D Phase Change

In Lagrangian description we have,

Energy equation:

$$\rho\frac{\partial e}{\partial t} + \boldsymbol{\nabla}\cdot\boldsymbol{q} = 0 \qquad \forall\ (\boldsymbol{x},t)\ \in\ \Omega_{xt} = \Omega_x \times \Omega_t = (0,1)\times(0,\tau) \tag{2.18}$$

Fourier heat conduction law:

$$\boldsymbol{q} = -k(T)\boldsymbol{\nabla}T \qquad \forall\ (\boldsymbol{x},t)\ \in\ \Omega_{xt} = \Omega_x \times \Omega_t = (0,1)\times(0,\tau) \tag{2.19}$$

Specific total energy *e*:

$$e = \int_{T_0}^{T} c_p(T)dT + L_f(T) \tag{2.20}$$

in which,

$$L_f(T) = \begin{cases} 0 & ; \quad T < T_s \\ L_f(T) & ; \quad T_s \le T \le T_l \\ L_f & ; \quad T > T_l \end{cases} \tag{2.21}$$

$$k(T) = \begin{cases} k_s & ; \quad T < T_s \\ k(T) & ; \quad T_s \le T \le T_l \\ k_l & ; \quad T > T_l \end{cases} \tag{2.22}$$

$$c_p(T) = \begin{cases} c_{ps} & ; \quad T < T_s \\ c_p(T) & ; \quad T_s \le T \le T_l \\ c_{pl} & ; \quad T > T_l \end{cases} \tag{2.23}$$

Case (a): Mathematical model containing higher order derivatives of the dependent variable *T*

Substituting from (2.19) and (2.20) in (2.18),

$$\rho c_p(T)\frac{\partial T}{\partial t} + \boldsymbol{\nabla}\cdot(-k(T)\boldsymbol{\nabla}T) + \rho\frac{\partial L_f}{\partial t} = 0 \tag{2.24}$$

$$L_f = L_f(T) \tag{2.25}$$

in which,

$$\frac{\partial L_f}{\partial t} = \frac{\partial L_f}{\partial T}\frac{\partial T}{\partial t} \tag{2.26}$$

If we consider a 1D case then,

$$\boldsymbol{\nabla} = \frac{\partial}{\partial x} \tag{2.27}$$

Hence, (2.24) can be written as,

$$\rho c_p(T)\frac{\partial T}{\partial t} + \frac{\partial}{\partial x}\left(-k(T)\frac{\partial T}{\partial x}\right) + \rho\frac{\partial L_f}{\partial T}\frac{\partial T}{\partial t} = 0 \tag{2.28}$$

$$L_f = L_f(T) \tag{2.29}$$

Once we define $L_f(T)$, $\frac{\partial L_f}{\partial T}$ is explicitly deterministic. Thus (2.28) is a single PDE in temperature that defines 1D phase change with smooth interface. We remark that $\frac{\partial L_f}{\partial T}\frac{\partial T}{\partial t}$ term is only to be used for $T_s \leq T \leq T_l$, otherwise it is zero. The conduction term in (2.28) can be further expanded,

$$\rho c_p(T)\frac{\partial T}{\partial t} - \frac{\partial k(T)}{\partial x}\frac{\partial T}{\partial x} - k(T)\frac{\partial^2 T}{\partial x^2} + \rho\frac{\partial L_f}{\partial T}\frac{\partial T}{\partial t} = 0 \tag{2.30}$$

Furthermore,

$$\frac{\partial k(T)}{\partial x} = \frac{\partial k(T)}{\partial T}\frac{\partial T}{\partial x} \tag{2.31}$$

Thus finally we have,

$$\rho c_p(T)\frac{\partial T}{\partial t} - \frac{\partial k(T)}{\partial T}\left(\frac{\partial T}{\partial x}\right)^2 - k(T)\frac{\partial^2 T}{\partial x^2} + \rho\frac{\partial L_f}{\partial T}\frac{\partial T}{\partial t} = 0 \tag{2.32}$$

in which,

$$\frac{\partial L_f}{\partial T}\frac{\partial T}{\partial t}\begin{cases} = 0 & ; \quad T < T_s \ ; \ T > T_l \\ \neq 0 & ; \quad T_s \leq T \leq T_l \ \text{ and deterministic using } L_f = L_f(T) \end{cases} \tag{2.33}$$

The mathematical model (2.32) contains only one dependent variable, T, the temperature and is most meritorious in terms of computational efficiency.

Case (b): Mathematical model consisting of a system of first order PDEs

The mathematical model (2.32) can be recast in terms of a system of first order PDEs using auxiliary variables and auxiliary equations. This form of the mathematical model is useful and is necessitated in finite element processes based on STLSP using local approximations of the class C^0 in space and time. If we define,

$$q = -k(T)\frac{\partial T}{\partial x} \tag{2.34}$$

and maintain the time derivative of L_f in (2.32), then we have the following system of first order PDEs in T, q, and L_f.

$$\rho c_p(T)\frac{\partial T}{\partial t} + \frac{\partial q}{\partial x} + \rho\frac{\partial L_f}{\partial t} = 0 \tag{2.35}$$

$$q + k(T)\frac{\partial T}{\partial x} = 0 \tag{2.36}$$

$$L_f - F(T) = 0 \tag{2.37}$$

in which q and L_f are auxiliary variables and (2.36) and (2.37) are auxiliary equations. $F(T)$ is the specification of $L_f(T)$ (see chapter 4 on numerical studies).

2.5.2 Mathematical Models for 2D Phase Change

For two dimensional spatial domain (2.18) - (2.25) hold, but $\boldsymbol{\nabla}$ is defined by,

$$\boldsymbol{\nabla} = \begin{bmatrix} \dfrac{\partial}{\partial x} & \dfrac{\partial}{\partial y} \end{bmatrix}^T \tag{2.38}$$

Hence we have the following mathematical models parallel to 1D case for homogeneous isotropic medium.

Case (a): Mathematical model containing higher order derivatives of the dependent variable *T*

Substituting for $\boldsymbol{\nabla}$ from (2.38) into (2.24),

$$\rho c_p(T)\frac{\partial T}{\partial t} + \frac{\partial}{\partial x}\left(-k(T)\frac{\partial T}{\partial x}\right) + \frac{\partial}{\partial y}\left(-k(T)\frac{\partial T}{\partial y}\right) + \rho\frac{\partial L_f}{\partial T}\frac{\partial T}{\partial t} = 0 \tag{2.39}$$

$$L_f - F(T) = 0 \tag{2.40}$$

T is the only dependent variable. (2.40) permits explicit expression for $\frac{\partial L_f}{\partial T}$ needed in (2.39). We remark that (2.33) must hold in this case as well.

Case (b): Mathematical model consisting of a system of first order PDEs

Following 1D case, we introduce q_x and q_y as auxiliary variables and maintain L_f as a dependent variable (for convenience) in the energy equation. This yields the following mathematical model.

$$\rho c_p(T)\frac{\partial T}{\partial t} + \frac{\partial q_x}{\partial x} + \frac{\partial q_y}{\partial y} + \rho\frac{\partial L_f}{\partial t} = 0 \tag{2.41}$$

$$q_x + k(T)\frac{\partial T}{\partial x} = 0 \tag{2.42}$$

$$q_y + k(T)\frac{\partial T}{\partial y} = 0 \tag{2.43}$$

$$L_f - F(T) = 0 \tag{2.44}$$

Here also, $F(T)$ is specification of $L_f(T)$. The conditions (2.33) apply in this case also.

Chapter 3

Methods of Approximation for IVPs Describing Phase Change Phenomena

3.1 Introduction

The mathematical models describing the phase change phenomena consist of a system of non-linear PDEs in spatial coordinates and time i.e. non-linear IVPs in which the space-time differential operator is non-linear. The computational methodology for obtaining numerical solutions of the IVPs i.e. evolution must be such that accurate numerical solutions are possible upon convergence. In the following, we list some features that are essential in choosing a computational methodology for obtaining numerical solutions of the non-linear IVPs describing phase change phenomena.

(1) Must be applicable to non-linear space-time differential operators regardless of the nature of the non-linearity without any ad-hoc adjustments or treatments that are dependent on the nature of the non-linearity (such as SUPG, DC, LS and other up-

winding methods and linearizing methods [10]).

(2) The dependent variables must exhibit simultaneous dependence on space coordinates and time as necessitated by the physics. Hence the computational methodology must only entertain a space-time coupled approach.

(3) Must yield a computational infrastructure in which the computations remain unconditionally stable regardless of the choices of computational or physical parameters. This feature essentially requires that the algebraic systems resulting from the methods of approximation must contain positive definite coefficient matrices.

(4) The approximation must be of higher degree (polynomial of order p) as well as of higher order in space and in time. These features allow simulation of complex evolution over larger sub-domains. The higher order feature of the approximation permits us to incorporate the desired global differentiability of approximations in space and time.

(5) The computational infrastructure must be time marching so that the evolution can be computed for an increment of time and then time marched to obtain the entire evolution. This feature is essential for efficiency of computations when evolution may be needed for a large value of time with relatively small time increments.

(6) The computational method must have means of measuring (i.e. computing) the error or residual without the knowledge of theoretical or reference solution and must also have mechanism to reduce them to the desired level. This feature is also essential for adaptivity.

Based on the material presented in Chapter 1 and the requirements (1) - (6), we rule out finite difference and finite volume methods as viable computational methodologies. This leaves us with space-time coupled finite element methods as possible approaches for obtaining numerical solutions of the IVPs in phase change phenomena.

3.2 Space-Time Finite Element Method

In space-time finite element methods we construct an integral form using the GDEs in the mathematical model over the space-time domain of the IVP. This can be done in two ways: (i) using fundamental lemma of the calculus of variations [17–21] or (ii) based on the minimization of the residual functional. The use of fundamental lemma results in space-time Galerkin Method (STGM), space-time Petrov-Galerkin method (STPGM) and space-time weighted residuals method (STWRM). The choice of the test function determines the type of method. If we begin with STGM and perform integration by parts, we obtain the weak form i.e. we have space-time Galerkin Method with weak form (STGM/WF). The second category of methods based on minimization of the residual functional results in space-time least squares processes (STLSP). When these space-time integral forms are recast over the space-time discretization of the space time domain, we have space-time finite element processes based on the chosen strategy of constructing the integral form. We note that these methods only provide the space-time integral form from which numerical solution is computed, thus we only have necessary condition. Existence and sufficient conditions in these methods must be addressed on problem by problem basis.

Surana et. al. [11, 12, 22] have shown that:

(i) All space-time differential operators can be classified into two mathematical cate-

gories: non-self adjoint and non-linear.

(ii) By establishing a correspondence between the integral forms and the elements of calculus of variations and by introducing the definition of space-time variationally consistent integral forms (STVC) and space-time variationally inconsistent integral forms (STVIC), it is possible to determine which space-time integral forms are STVC or STVIC for the two categories of differential operators.

(iii) The STVC integral forms yield computational processes that are unconditionally stable. The coefficient matrices in the algebraic systems are symmetric and positive definite. In case of STVIC integral forms, unconditional stability of computations is not always ensured, the coefficient matrices in the algebraic system are not symmetric, and hence their positive definiteness is not always ensured.

(iv) The STGM, STPGM, STWRM, and STGM/WF yield space-time variationally inconsistent integral forms. STLSP yield STVC integral forms when the space-time differential operator is non-self adjoint. When the space-time differential operator is non-linear, the space-time integral form in STLSP can be made variationally consistent if (a) the non-linear algebraic equations are solved using Newton's linear method (Newton-Raphson method) and (b) if the second variation of the residuals is neglected in the second variation of the residual functional.

Based on these works described above, only STLSP are a viable computational strategy for obtaining numerical solutions of the IVPs describing the evolution for phase change phenomena. This approach also has all of the desired features (1) - (6) listed in section 3.1. In the following, we consider STLSP for IVPs in which the space-time differential operator is non-linear. First, we give a general presentation followed by specific details of the

formulations using the mathematical models (presented in Chapter 2) used in the present work for computations.

3.2.1 Space-time Finite Element Least Squares Processes for Non-linear Space-time Differential Operators [11, 12, 22]

Let

$$\boldsymbol{A\phi} - \boldsymbol{f} = 0 \qquad \forall\ (\boldsymbol{x}, t)\ \in\ \Omega_{xt} = \Omega_x \times \Omega_t = \Omega_x \times (0, \tau) \tag{3.1}$$

be a system of n_e partial differential equations defined over the space-time domain Ω_{xt}. $\boldsymbol{A}$ is a $n_e \times n_e$ matrix containing n_e differential operators and $\boldsymbol{\phi}$ is a $(n_e \times 1)$ vector of dependent variables. Consider an increment of time $\Delta t = [t_n, t_{n+1}]$ i.e. $\Omega_t^n = (t_n, t_{n+1})$ and the n^{th} space-time strip or slab $\Omega_{xt}^n = \Omega_x \times \Omega_t^n = \Omega_x \times (t_n, t_{n+1})$ corresponding to this increment of time. Let $(\Omega_{xt}^n)^T$ be a discretization of Ω_{xt}^n, the n^{th} space-time strip or slab such that,

$$\left(\bar{\Omega}_{xt}^n\right)^T = \bigcup_{e=1}^{m} \Omega_{xt}^e \tag{3.2}$$

in which $\bar{\Omega}_{xt}^n = \Omega_{xt}^n \bigcup \Gamma^n$ where Γ^n is the closed boundary of the n^{th} space-time strip or slab. $\bar{\Omega}_{xt}^e = \Omega_{xt}^e \bigcup \Gamma^e$ is a typical space-time element 'e' of the discretization $(\Omega_{xt}^n)^T$. Γ^e is the closed boundary of element 'e'. Let $\boldsymbol{\phi}_h$ be approximation of $\boldsymbol{\phi}$ over $(\Omega_{xt}^n)^T$ and $\boldsymbol{\phi}_h^e$ be local approximation of $\boldsymbol{\phi}$ over an element 'e' with space-time domain $\bar{\Omega}_{xt}^e$ such that,

$$\boldsymbol{\phi}_h = \bigcup_{e=1}^{m} \boldsymbol{\phi}_h^e \tag{3.3}$$

If we substitute $\boldsymbol{\phi}_h$ in (3.1) then we obtain 'n_e' residual equations i.e.

$$\boldsymbol{A\phi}_h - \boldsymbol{f} = \boldsymbol{E} \tag{3.4}$$

The vector $\boldsymbol{E}$ consists of E_i ; $i = 1, ..., n_e$ residual equations.

1. Existence of the residual functional $I(\boldsymbol{\phi}_h)$:

$$I(\boldsymbol{\phi}_h) = \sum_{i=1}^{n_e} (E_i, E_i)_{\left(\bar{\Omega}_{xt}^n\right)^T} = \sum_{e=1}^{m} \left(\sum_{i=1}^{n_e} (E_i^e, E_i^e)_{\bar{\Omega}_{xt}^e} \right) \tag{3.5}$$

in which E_i^e are components of the vector $\boldsymbol{E}^e$ in

$$\boldsymbol{A}\boldsymbol{\phi}_h^e - \boldsymbol{f} = \boldsymbol{E}^e \tag{3.6}$$

We note $I(\boldsymbol{\phi}_h)$ is always greater than zero and is equal to zero iff $\boldsymbol{\phi}_h = \boldsymbol{\phi}$, the theoretical solution of (3.1).

2. Necessary Condition:

$$\delta I(\boldsymbol{\phi}_h) = 2\sum_{e=1}^{m} \left(\sum_{i=1}^{n_e} (E_i^e, \delta E_i^e)_{\bar{\Omega}_{xt}^e} \right) = 2\sum_{e=1}^{m} \{g^e\} = 2\{g\} = 0 \tag{3.7}$$

We note that $\{g^e\}$ is a non-linear function of $\boldsymbol{\phi}_h^e$ and likewise $\{g\}$ is a non-linear function of $\boldsymbol{\phi}_h$.

3. Sufficient condition or extremum principle:

$$\delta^2 I(\boldsymbol{\phi}_h) = 2\sum_{e=1}^{m} \left(\sum_{i=1}^{n_e} (\delta E_i^e, \delta E_i^e)_{\bar{\Omega}_{xt}^e} \right) + 2\sum_{e=1}^{m} \left(\sum_{i=1}^{n_e} \left(E_i^e, \delta^2 E_i^e\right)_{\bar{\Omega}_{xt}^e} \right) \tag{3.8}$$

A unique extremum principle requires

$$\delta^2 I \begin{cases} > 0 \quad ; \quad \text{minimum of } I \\ = 0 \quad ; \quad \text{saddle point of } I \qquad \forall \text{ admissible } \boldsymbol{\phi}_h \\ < 0 \quad ; \quad \text{maximum of } I \end{cases} \tag{3.9}$$

When the differential operator is linear (non-self adjoint), $\delta^2 E_i^e = 0$, $i = 1, 2, ..., n_e$. Hence $\delta^2 I(\boldsymbol{\phi}_h) > 0$ holds in (3.8). Thus, in this case, we have a unique extremum principle and based on (3.9), hence a $\boldsymbol{\phi}_h$ obtained using (3.7) minimizes $I(\boldsymbol{\phi}_h)$ in (3.5). When the

differential operator is non-linear $\delta^2 E_i^e$ are not zero, hence (3.7) in its present form does not satisfy any of the three conditions in (3.9), thus we do not have an extremum principle. This situation can be corrected by a simple modification. We note that $\delta I\left(\boldsymbol{\phi}_h\right) = 0$ yields $\big($from (3.7)$\big)$,

$$\{g\} = \{g\left(\boldsymbol{\phi}_h\right)\} = 0 = \sum_{e=1}^{m} \left(\sum_{i=1}^{n_e} \left(E_i^e, \delta E_i^e\right)_{\bar{\Omega}_{xt}^e} \right) \tag{3.10}$$

Consider local approximations for the dependent variables $\boldsymbol{\phi}$ i.e. $\boldsymbol{\phi}_h^e$. Each dependent variable in $\boldsymbol{\phi}$ has its own local approximation. Collectively they constitute $\boldsymbol{\phi}_h^e$. Let all of the degrees of freedom in the local approximation $\boldsymbol{\phi}_h^e$ be $\{\delta^e\}$ and let

$$\{\delta\} = \bigcup_{e=1}^{m} \{\delta^e\} \tag{3.11}$$

be the degrees of freedom for the discretization $\left(\bar{\Omega}_{xt}^n\right)^T$, then $\{g\}$ in (3.10) is a non-linear function of $\{\delta\}$ i.e. we must find $\{\delta\}$ that satisfies,

$$\{g\left(\{\delta\}\right)\} = 0 \tag{3.12}$$

iteratively. We choose Newton's linear method (Newton-Raphson method). Let $\{\delta^0\}$ be an assumed solution or guess of $\{\delta\}$ in (3.12). Then,

$$\{g\left(\{\delta^0\}\right)\} \neq 0 \tag{3.13}$$

Let $\{\Delta\delta\}$ be a change in $\{\delta^0\}$ such that,

$$\{g\left(\{\delta^0\} + \{\Delta\delta\}\right)\} = 0 \tag{3.14}$$

Expanding $\{g\left(\{\delta^0\} + \{\Delta\delta\}\right)\}$ in Taylor series about $\{\delta^0\}$ and retaining only up to linear terms in $\{\Delta\delta\}$ yields,

$$\{g\left(\{\delta^0\} + \{\Delta\delta\}\right)\} \approx \{g\left(\{\delta^0\}\right)\} + \left.\frac{\partial\{g\}}{\partial\{\delta\}}\right|_{\{\delta^0\}} \{\Delta\delta\} = 0 \tag{3.15}$$

From (3.15), we can solve for $\{\Delta\delta\}$.

$$\{\Delta\delta\} = -\left[\frac{\partial\{g\}}{\partial\{\delta\}}\right]^{-1}_{\{\delta^0\}} \{g\left(\{\delta^0\}\right)\} \tag{3.16}$$

We note that,

$$\frac{\partial\{g\}}{\partial\{\delta\}} = \delta\{g\} = \sum_{e=1}^{m}\left(\sum_{i=1}^{n_e}\left(\delta E_i^e, \delta E_i^e\right)_{\bar{\Omega}_{xt}^e}\right) + \sum_{e=1}^{m}\left(\sum_{i=1}^{n_e}\left(E_i^e, \delta^2 E_i^e\right)_{\bar{\Omega}_{xt}^e}\right) = \frac{1}{2}\delta^2 I\left(\boldsymbol{\phi}_h\right) \tag{3.17}$$

If $\left[\frac{\partial\{g\}}{\partial\{\delta\}}\right]$ is positive definite in (3.16), then we can ensure a unique solution $\{\Delta\delta\}$ from (3.16). Based on (3.17) this is possible if we approximate $\delta^2 I\left(\phi_h\right)$ by [9, 11, 12, 22–25],

$$\delta^2 I\left(\boldsymbol{\phi}_h\right) \approx 2\sum_{e=1}^{m}\left(\sum_{i=1}^{n_e}\left(\delta E_i^e, \delta E_i^e\right)_{\bar{\Omega}_{xt}^e}\right) > 0 \text{ , a unique extremum principle.} \tag{3.18}$$

Rationale for the approximation in (3.18) has been discussed by Surana et. al. [9, 11, 12, 22–25]. Thus, with (3.18) STLSP is STVC.

Once we find a $\{\Delta\delta\}$ using (3.16) and (3.18), it is helpful to consider the following for obtaining an updated solution $\{\delta\}$,

$$\{\delta\} = \{\delta^0\} + \alpha\{\Delta\delta\} \tag{3.19}$$

in which α is a scalar generally between 0 and 2 and assumes the largest value between 0 and 2 for which $I\left(\{\delta\}\right) \leq I\left(\{\delta^0\}\right)$ holds. This is referred to as line search. The entire process of solving for $\{\Delta\delta\}$ and to update $\{\delta^0\}$ to obtain $\boldsymbol{\phi}_h$ that satisfies $\{g\left(\{\delta\}\right)\} = 0$ is called Newton's method with line search.

In (3.17), we note that,

$$[K^e] = \sum_{i=1}^{n_e}\left(\delta E_i^e, \delta E_i^e\right)_{\bar{\Omega}_{xt}^e} \tag{3.20}$$

is in fact the element coefficient matrix and,

$$\sum_{e=1}^{m}\left(\sum_{i=1}^{n_e}\left(\delta E_i^e, \delta E_i^e\right)_{\bar{\Omega}_{xt}^e}\right) = \sum_{e=1}^{m}[K^e] = [K] \tag{3.21}$$

is the process of assembly of the element matrices. The same holds true for $\{g\}$ and $\{g^e\}$ in (3.7). We note that the computation of $\{g^e\}$ and $[K^e]$ needed in (3.16) requires E_i^e; $i = 1, 2, ..., n_e$ and δE_i^e; $i = 1, 2, ..., n_e$. Once we have $[K^e]$ and $\{g^e\}$, we assemble them and solve for $\{\Delta\delta\}$ using (3.16) followed by an updated $\{\delta\}$ using (3.19). Using a new $\{\delta\}$ we check if $|\{g(\{\delta\})\}| \leq \Delta$ holds, in which Δ is a preset tolerance, a threshold value of numerically computed zero. If not, we repeat the process by taking the new $\{\delta\}$ as $\{\delta^0\}$.

3.2.2 Summary of Computational Steps and Time-Marching Procedure

In the following we list important computational steps in the STLSP and the time marching procedure for computing the complete evolution.

1. Consider PDEs in the mathematical model (either a higher order system or a system of first order PDEs) and identify dependent variables. The mathematical model obviously must have closure.

2. Consider the first space-time strip or slab for an increment of time and its spatial discretization into space-time finite elements, generally nine-node p-version elements (in x, t) or 27-node p-version elements (in x, y, and t) with higher order continuity local approximations in space and time.

3. Consider local approximations for each dependent variable. p-level and the order of space $k = (k_1, k_2)$ (in space and time) can be different for each dependent variable. Minimally conforming choice of k is dependent on the highest orders of the derivatives in space and time for each dependent variable and whether the integrals are in

Riemann or Lebesque sense.

4. Arrange nodal degrees of freedom for each variable as a vector and then arrange them in a single vector $\{\delta^e\}$ representing all degrees of freedom for all of the dependent variables for an element 'e'. Thus we have $\{\delta^e\}$ as nodal degrees of freedom for each element and,

$$\{\delta\} = \bigcup_{e=1}^{m} \{\delta^e\} \tag{3.22}$$

where $\{\delta\}$ are the total degrees of freedom for the entire discretization for the first space-time strip or slab.

5. Assume a starting solution $\{\delta^0\}$ for $\{\delta\}$.

6. Using local approximation for each dependent variable compute,

$$\{g^e\} = \sum_{i=1}^{n_e} (E_i^e, \delta E_i^e)_{\bar{\Omega}_{xt}^e} \quad ; \quad e = 1, 2, ..., m \tag{3.23}$$

$$[K^e] = \sum_{i=1}^{n_e} (\delta E_i^e, \delta E_i^e)_{\bar{\Omega}_{xt}^e} \quad ; \quad e = 1, 2, ..., m \tag{3.24}$$

$$[I^e] = \sum_{i=1}^{n_e} (E_i^e, E_i^e)_{\bar{\Omega}_{xt}^e} \quad ; \quad e = 1, 2, ..., m \tag{3.25}$$

7. Assemble $\{g^e\}$ and $[K^e]$ to obtain $\{g\}$ and $[K]$ i.e

$$\{g\} = \sum_{e=1}^{m} \{g^e\} \tag{3.26}$$

$$[K] = \sum_{e=1}^{m} [K^e] \tag{3.27}$$

$$I = \sum_{e=1}^{m} I^e \tag{3.28}$$

8. Use

$$\{\Delta\delta\} = -[K]^{-1} \{g\} \tag{3.29}$$

to calculate $\{\Delta\delta\}$ after imposing boundary conditions (BCs) and initial conditions (ICs) on $\{\delta\}$.

9. Find new updated solution using,

$$\{\delta\} = \{\delta^0\} + \alpha\{\Delta\delta\} \qquad ; \quad 0 < \alpha \leq 2 \text{ such that } I\left(\{\delta\}\right) \leq I\left(\{\delta^0\}\right) \tag{3.30}$$

10. Recalculate $\{g^e\}$ using (3.25) and updated $\{\delta\}$. Assemble $\{g^e\}$ to obtain $\{g\}$ as in (3.26). Check if the absolute value of each component of $\{g\}$ is less than or equal to Δ, a preset threshold value for numerically computed zero (generally 10^{-6} or lower suffices).

    If this condition is satisfied then we have a solution of the non-linear algebraic system defined by $\{g\}$ and we say that Newton's linear method is converged. If not, then reset $\{\delta^0\}$ to $\{\delta\}$ and repeat steps 6 through 10 until convergence of the Newton's linear method is achieved.

The steps described here provide a solution for the first space-time strip or slab between $t = 0$ and $t = \Delta t$. Next, consider the second space-time strip between $t = \Delta t$ and $t = 2\Delta t$. Initial conditions for this space-time strip or slab are obtained from the solution for the first space-time strip or slab at $t = \Delta t$. Repeat the same procedure as used for the first space-time strip or slab. This procedure known as 'time marching procedure' can be continued until the desired time is reached.

We remark that E_i^e, I^e, and I are scalars, δE_i^e are vectors and hence $\{g^e\}$ are also vectors but $(\delta E_i^e, \delta E_i^e)_{\bar{\Omega}_{xt}^e}$ is a matrix. Thus, care must be taken in various scalar products encountered in the space-time least squares finite element process described in this section.

3.3 Details of Space-Time Least Squares Finite Element Process for the Specific Mathematical Models

In this section we consider the mathematical models presented in Chapter 2 and provide specific details of the space-time least squares finite element processes. We consider 1D and 2D mathematical models proposed in this work (both forms of GDEs) and 1D phase field mathematical model.

3.3.1 1D Mathematical Models Used in the Present Work

Case (a): Mathematical model containing higher order derivatives of the dependent variable *T*

In this case the mathematical model consists of (2.30) to (2.33),

$$\rho c_p(T)\frac{\partial T}{\partial t} - \frac{\partial k(T)}{\partial x}\frac{\partial T}{\partial x} - k(T)\frac{\partial^2 T}{\partial x^2} + \rho\frac{\partial L_f}{\partial T}\frac{\partial T}{\partial t} = 0 \tag{3.31}$$

where,

$$L_f = L_f(T) \quad ; \quad \text{known function} \tag{3.32}$$

Let

$$T_h^e \in V_h \subset H^{k,p}\left(\bar{\Omega}_{xt}^e\right) \tag{3.33}$$

where $k = (k_1, k_2)$, $p = (p_1, p_2)$;$p_1 \geq 2k_1 - 1$, $p_2 \geq 2k_2 - 1$. k_1 and k_2 are the orders of the space in space and time and p_1, p_2 are the degrees of local approximation in space and time. $k_1 = 3$ and $k_2 = 2$ correspond to the minimally conforming approximation space for

which the integrals over $\left(\bar{\Omega}_{xt}^{n}\right)^{T}$ are in Riemann sense. If we choose $k_1 = 2$ and $k_2 = 1$, then the integrals over $\left(\bar{\Omega}_{xt}^{n}\right)^{T}$ will be in Lebesque sense. Let

$$T_h^e = \sum_{i=1}^{n} N_i(x,t) T_i^e = [N]\{T^e\} = [N]\{\delta^e\} \tag{3.34}$$

be the local approximation for T over $\bar{\Omega}_{xt}^{e}$. If we choose,

$$N_i \in V_h \subset H^{k,p}\left(\bar{\Omega}_{xt}^{e}\right) ; i = 1, 2, ..., n \tag{3.35}$$

then (3.33) will hold. Substituting T_h^e from (3.34) into (3.31) we obtain the residual equation for an element 'e'.

$$E^e = \rho c_p\left(T_h^e\right)\frac{\partial T_h^e}{\partial t} - \frac{\partial k\left(T_h^e\right)}{\partial T}\left(\frac{\partial T_h^e}{\partial x}\right)^2 - k\left(T_h^e\right)\frac{\partial^2 T_h^e}{\partial x^2} + \rho\frac{L_f\left(T_h^e\right)}{\partial T}\frac{\partial T_h^e}{\partial t} \qquad \forall\ (x,t) \in \bar{\Omega}_{xt}^{e} \tag{3.36}$$

and,

$$L_f\left(T_h^e\right) = F\left(T_h^e\right) \qquad \text{; with the restriction (2.33)} \tag{3.37}$$

Next we need δE^e i.e. $\frac{\partial E^e}{\partial\{\delta^e\}}$. Using (3.36) we can write,

$$\begin{aligned}\delta E^e = \left\{\frac{\partial E^e}{\partial\{\delta^e\}}\right\} =& \rho\frac{\partial c_p\left(T_h^e\right)}{\partial T}\{N\}\frac{\partial T_h^e}{\partial t} + \rho c_p\left(T_h^e\right)\left\{\frac{\partial N}{\partial t}\right\} \\ &- \frac{\partial^2 k\left(T_h^e\right)}{\partial T^2}\{N\}\left(\frac{\partial T_h^e}{\partial x}\right)^2 - 2\frac{\partial k\left(T_h^e\right)}{\partial T}\left\{\frac{\partial N}{\partial x}\right\}\frac{\partial T_h^e}{\partial x} \\ &- \frac{\partial k\left(T_h^e\right)}{\partial T}\{N\}\frac{\partial^2 T_h^e}{\partial x^2} - k\left(T_h^e\right)\left\{\frac{\partial^2 N}{\partial x^2}\right\} \\ &+ \frac{\partial^2 L_f\left(T_h^e\right)}{\partial T^2}\{N\}\frac{\partial T_h^e}{\partial t} + \rho\frac{\partial L_f\left(T_h^e\right)}{\partial T}\left\{\frac{\partial N}{\partial t}\right\}\end{aligned} \tag{3.38}$$

With E^e and δE^e given by (3.36) and (3.38), then $\{g^e\}$ and $[K^e]$ are defined. Except in the phase change transition zone, k and c_p are constant and hence their derivative with respect to temperature are zero and $\frac{\partial L_f(T)}{\partial T}$ is zero outside the transition region. We note that

$$\{g^e\} = \left(E^e, \delta E^e\right)_{\bar{\Omega}_{xt}^{e}} = \int_{\bar{\Omega}_{xt}^{e}} E^e\left\{\frac{\partial E^e}{\partial\{\delta^e\}}\right\} d\Omega_{xt} \tag{3.39a}$$

and,

$$[K^e] = (\delta E^e, \delta E^e)_{\bar{\Omega}^e_{xt}} = \int_{\bar{\Omega}^e_{xt}} \left\{ \frac{\partial E^e}{\partial \{\delta^e\}} \right\} \left\{ \frac{\partial E^e}{\partial \{\delta^e\}} \right\}^T d\Omega_{xt} \tag{3.39b}$$

Gauss quadrature is used to compute numerical values of $\{g^e\}$ and $[K^e]$. We remark that approximation functions in (3.34) are shown to be functions of x and t for convenience. The elements are mapped in the natural coordinate space (ξ, η). The natural coordinate space is used for defining N_i's as well as all computations. Details are standard [26] and hence omitted.

Case (b): 1D Mathematical model as a system of first order PDEs used in the present work

Following the derivation in Chapter 2, in this case we have,

$$\rho c_p(T) \frac{\partial T}{\partial t} + \frac{\partial q}{\partial x} + \rho \frac{\partial L_f}{\partial t} = 0 \tag{3.40}$$

$$q + k(T) \frac{\partial T}{\partial x} = 0 \tag{3.41}$$

$$L_f - F(T) = 0 \quad \text{; known function} \quad \forall\, T \in [T_s, T_l] \tag{3.42}$$

we treat T, q, and L_f as dependent variables.

Let T^e_h, q^e_h, and $(L_f)^e_h$ be the local approximations for T, q, and L_f over a space-time element $\bar{\Omega}^e_{xt}$.

$$T^e_h = \left[N^T\right] \{T^e\} \tag{3.43}$$

$$q^e_h = [N^q] \{q^e\} \tag{3.44}$$

$$(L_f)^e_h = \left[N^{L_f}\right] \{(L_f)^e\} \tag{3.45}$$

Each dependent variable has its own local approximation functions and nodal degrees of freedom. Let

$$\{\delta^e\}^T = \left[\{T^e\}^T, \{q^e\}^T, \{(L_f)^e\}^T\right] \tag{3.46}$$

be the total degrees of freedom for all three dependent variables. Since the PDEs contain only the first order derivatives T, q, and L_f in space and time we can choose the same approximation space for N_i^T, N_i^q, $N_i^{L_f}$ i.e.

$$\begin{aligned} N_i^T \ &\in \ V_h \ \subset \ H^{k,p}\left(\bar{\Omega}_{xt}^e\right) \quad ; \quad i = 1, 2, ..., n_T \\ N_i^q \ &\in \ V_h \ \subset \ H^{k,p}\left(\bar{\Omega}_{xt}^e\right) \quad ; \quad i = 1, 2, ..., n_q \\ N_i^{L_f} \ &\in \ V_h \ \subset \ H^{k,p}\left(\bar{\Omega}_{xt}^e\right) \quad ; \quad i = 1, 2, ..., n_{L_f} \end{aligned} \tag{3.47}$$

in which $k = (k_1, k_2)$, $p = (p_1, p_2)$; $p_1 \geq 2k_1 - 1$, $p_2 \geq 2k_2 - 1$. $k_1 = 2$ and $k_2 = 2$ correspond to the minimally conforming space if the space-time integrals over $\left(\bar{\Omega}_{xt}^n\right)^T$ are considered in Riemann sense. The choices $k_1 = 1$ and $k_2 = 1$ would yield integrals over $\left(\bar{\Omega}_{xt}^n\right)^T$ in Lebesque sense. n_T, n_q, and n_{L_f} are degrees of freedom for T_h^e, q_h^e, and $(L_f)_h^e$ are in V_h space. Substituting from (3.43) - (3.45) into (3.40) - (3.42) we obtain the following residual equations.

$$\left.\begin{aligned} E_1^e &= \rho c_p \left(T_h^e\right) \frac{\partial T_h^e}{\partial t} + \frac{\partial q_h^e}{\partial x} + \rho \frac{\partial \left(L_f\right)_h^e}{\partial t} \\ E_2^e &= q_h^e + k\left(T_h^e\right) \frac{\partial T_h^e}{\partial x} \\ E_3^e &= \left(L_f\right)_h^e - F\left(T_h^e\right) \end{aligned}\right\} \quad \forall \ (x,t) \ \in \ \bar{\Omega}_{xt}^e \tag{3.48}$$

Next, we determine variations of $E_i^e \quad ; \quad i = 1, 2, 3.$

$$\delta E_1^e = \left\{\frac{\partial E_1^e}{\partial\{\delta^e\}}\right\} = \begin{Bmatrix} \left\{\frac{\partial E_1^e}{\partial\{T^e\}}\right\} \\ \left\{\frac{\partial E_1^e}{\partial\{q^e\}}\right\} \\ \left\{\frac{\partial E_1^e}{\partial\{\left(L_f\right)^e\}}\right\} \end{Bmatrix} = \begin{Bmatrix} \rho\frac{\partial c_p\left(T_h^e\right)}{\partial T}\{N^T\}\frac{\partial T_h^e}{\partial t} + \rho c_p\left(T_h^e\right)\left\{\frac{\partial N^T}{\partial t}\right\} \\ \left\{\frac{\partial N^q}{\partial x}\right\} \\ \left\{\rho\frac{\partial N^{L_f}}{\partial t}\right\} \end{Bmatrix} \tag{3.49}$$

$$\delta E_2^e = \left\{\frac{\partial E_2^e}{\partial\{\delta^e\}}\right\} = \begin{Bmatrix} \left\{\frac{\partial E_2^e}{\partial\{T^e\}}\right\} \\ \left\{\frac{\partial E_2^e}{\partial\{q^e\}}\right\} \\ \left\{\frac{\partial E_2^e}{\partial\{\left(L_f\right)^e\}}\right\} \end{Bmatrix} = \begin{Bmatrix} \frac{\partial k\left(T_h^e\right)}{\partial T}\{N^T\}\frac{\partial T_h^e}{\partial x} + k\left(T_h^e\right)\left\{\frac{\partial N^T}{\partial x}\right\} \\ \left\{N^q\right\} \\ \left\{0\right\} \end{Bmatrix} \tag{3.50}$$

$$\delta E_3^e = \left\{\frac{\partial E_3^e}{\partial\{\delta^e\}}\right\} = \begin{Bmatrix} \left\{\frac{\partial E_3^e}{\partial\{T^e\}}\right\} \\ \left\{\frac{\partial E_3^e}{\partial\{q^e\}}\right\} \\ \left\{\frac{\partial E_3^e}{\partial\{\left(L_f\right)^e\}}\right\} \end{Bmatrix} = \begin{Bmatrix} -\frac{\partial F\left(T_h^e\right)}{\partial T}\{N^T\} \\ \left\{0\right\} \\ \left\{N^{L_f}\right\} \end{Bmatrix} \tag{3.51}$$

Hence,

$$\{g^e\} = \sum_{i=1}^{3}\left(E_i^e, \delta E_i^e\right)_{\bar{\Omega}_{xt}^e} = \sum_{i=1}^{3}\int_{\bar{\Omega}_{xt}^e} E_i^e\left\{\frac{\partial E_i^e}{\partial\{\delta^e\}}\right\} d\Omega_{xt} \tag{3.52}$$

and

$$[K^e] = \sum_{i=1}^{3}\left(\delta E_i^e, \delta E_i^e\right)_{\bar{\Omega}_{xt}^e} = \sum_{i=1}^{3}\int_{\bar{\Omega}_{xt}^e}\left\{\frac{\partial E_i^e}{\partial\{\delta^e\}}\right\}\left\{\frac{\partial E_i^e}{\partial\{\delta^e\}}\right\}^T d\Omega_{xt} \tag{3.53}$$

3.3.2 2D Mathematical Model as a System of First Order PDEs used in the Present Work

The details of the mathematical models in higher order derivatives of the temperature and the model as a system of first order PDEs are presented in Chapter 2 section 2.5.2. The details of the space-time LSP are exactly parallel to the 1D case except that in this case the space-time domain is x, y, and t i.e. a volume in x, y, t space. However for the sake of completeness we present details of the space-time least squares finite element process for the mathematical model that consists of a system of first order PDEs given by equations

(2.41) - (2.44), as it is used in the numerical studies.

$$\rho c_p(T)\frac{\partial T}{\partial t} + \frac{\partial q_x}{\partial x} + \frac{\partial q_y}{\partial y} + \rho\frac{\partial L_f}{\partial t} = 0 \tag{3.54}$$

$$q_x + k(T)\frac{\partial T}{\partial x} = 0 \tag{3.55}$$

$$q_y + k(T)\frac{\partial T}{\partial y} = 0 \tag{3.56}$$

$$L_f - F(T) = 0 \tag{3.57}$$

Let T_h^e, $(q_x)_h^e$, $(q_y)_h^e$, and $(L_f)_h^e$, be the local approximations for the dependent variables T, q_x, q_y, and L_f over $\bar{\Omega}_{xt}^e$.

$$T_h^e = \left[N^T\right]\{T^e\} \tag{3.58}$$

$$(q_x)_h^e = \left[N^{q_x}\right]\{q_x^e\} \tag{3.59}$$

$$(q_y)_h^e = \left[N^{q_y}\right]\{q_y^e\} \tag{3.60}$$

$$(L_f)_h^e = \left[N^{L_f}\right]\{(L_f)^e\} \tag{3.61}$$

Let

$$\{\delta^e\}^T = \left[\{T^e\}^T, \{q_x^e\}^T, \{q_y^e\}^T, \{(L_f)^e\}^T\right] \tag{3.62}$$

be the total degrees of freedom for an element 'e'. As before, in this case also N_i^T, $N_i^{q_x}$, $N_i^{q_y}$, $N_i^{L_f}$ are in approximation space $V_h \in H^{k,p}\left(\bar{\Omega}_{xt}^e\right)$. The minimally conforming k_1 and k_2 are clearly 2 and 2 for the integral over $\left(\bar{\Omega}_{xt}^n\right)^T$ to be Riemann. $k_1 = k_2 = 1$ i.e. solutions of class C^0 in space and time will obviously yield integrals over $\left(\bar{\Omega}_{xt}^n\right)^T$ in Lebesque sense. Substituting (3.58) - (3.61) into (3.54) - (3.57), we obtain residual equations for an element 'e',

$$\left.\begin{aligned} E_1^e &= \rho c_p\left(T_h^e\right)\frac{\partial T_h^e}{\partial t} + \frac{\partial\left(q_x\right)_h^e}{\partial x} + \frac{\partial\left(q_y\right)_h^e}{\partial y} + \rho\frac{\partial\left(L_f\right)_h^e}{\partial t} \\ E_2^e &= \left(q_x\right)_h^e + k\left(T_h^e\right)\frac{\partial T_h^e}{\partial x} \\ E_3^e &= \left(q_y\right)_h^e + k\left(T_h^e\right)\frac{\partial T_h^e}{\partial y} \\ E_4^e &= \left(L_f\right)_h^e - F\left(T_h^e\right) \end{aligned}\right\} \quad \forall\ (x,t)\ \in\ \bar{\Omega}_{xt}^e \tag{3.63}$$

The variations of E_i^e; i.e. $i = 1, 2, ..., 4$ are given by the following,

$$\delta E_1^e = \left\{\frac{\partial E_1^e}{\partial\{\delta^e\}}\right\} = \begin{Bmatrix} \left\{\frac{\partial E_1^e}{\partial\{T^e\}}\right\} \\ \left\{\frac{\partial E_1^e}{\partial\{q_x^e\}}\right\} \\ \left\{\frac{\partial E_1^e}{\partial\{q_y^e\}}\right\} \\ \left\{\frac{\partial E_1^e}{\partial\{\left(L_f\right)^e\}}\right\} \end{Bmatrix} = \begin{Bmatrix} \rho\frac{\partial c_p\left(T_h^e\right)}{\partial T}\{N^T\}\frac{\partial T_h^e}{\partial t} + \rho c_p\left(T_h^e\right)\left\{\frac{\partial N^T}{\partial t}\right\} \\ \left\{\frac{\partial N^{q_x}}{\partial x}\right\} \\ \left\{\frac{\partial N^{q_y}}{\partial y}\right\} \\ \left\{\rho\frac{\partial N^{L_f}}{\partial t}\right\} \end{Bmatrix} \tag{3.64}$$

$$\delta E_2^e = \left\{\frac{\partial E_2^e}{\partial\{\delta^e\}}\right\} = \begin{Bmatrix} \left\{\frac{\partial E_2^e}{\partial\{T^e\}}\right\} \\ \left\{\frac{\partial E_2^e}{\partial\{q_x^e\}}\right\} \\ \left\{\frac{\partial E_2^e}{\partial\{q_y^e\}}\right\} \\ \left\{\frac{\partial E_2^e}{\partial\{\left(L_f\right)^e\}}\right\} \end{Bmatrix} = \begin{Bmatrix} \frac{\partial k\left(T_h^e\right)}{\partial T}\{N^T\}\frac{\partial T_h^e}{\partial x} + k\left(T_h^e\right)\left\{\frac{\partial N^T}{\partial x}\right\} \\ \left\{N^{q_x}\right\} \\ \left\{0\right\} \\ \left\{0\right\} \end{Bmatrix} \tag{3.65}$$

$$\delta E_3^e = \left\{\frac{\partial E_3^e}{\partial\{\delta^e\}}\right\} = \begin{Bmatrix} \left\{\frac{\partial E_3^e}{\partial\{T^e\}}\right\} \\ \left\{\frac{\partial E_3^e}{\partial\{q_x^e\}}\right\} \\ \left\{\frac{\partial E_3^e}{\partial\{q_y^e\}}\right\} \\ \left\{\frac{\partial E_3^e}{\partial\{\left(L_f\right)^e\}}\right\} \end{Bmatrix} = \begin{Bmatrix} \frac{\partial k\left(T_h^e\right)}{\partial T}\{N^T\}\frac{\partial T_h^e}{\partial y} + k\left(T_h^e\right)\left\{\frac{\partial N^T}{\partial y}\right\} \\ \left\{0\right\} \\ \left\{N^{q_y}\right\} \\ \left\{0\right\} \end{Bmatrix} \tag{3.66}$$

$$\delta E_4^e = \left\{\frac{\partial E_4^e}{\partial\{\delta^e\}}\right\} = \begin{Bmatrix} \left\{\frac{\partial E_4^e}{\partial\{T^e\}}\right\} \\ \left\{\frac{\partial E_4^e}{\partial\{q_x^e\}}\right\} \\ \left\{\frac{\partial E_4^e}{\partial\{q_y^e\}}\right\} \\ \left\{\frac{\partial E_4^e}{\partial\{\left(L_f\right)^e\}}\right\} \end{Bmatrix} = \begin{Bmatrix} -\frac{\partial F\left(T_h^e\right)}{\partial T}\{N^T\} \\ \left\{0\right\} \\ \left\{0\right\} \\ \left\{N^{L_f}\right\} \end{Bmatrix} \tag{3.67}$$

Hence,

$$\{g^e\} = \sum_{i=1}^{4} (E_i^e, \delta E_i^e)_{\bar{\Omega}_{xt}^e} = \sum_{i=1}^{4} \int_{\bar{\Omega}_{xt}^e} E_i^e \left\{ \frac{\partial E_i^e}{\partial \{\delta^e\}} \right\} d\Omega_{xt} \tag{3.68}$$

and

$$[K^e] = \sum_{i=1}^{4} (\delta E_i^e, \delta E_i^e)_{\bar{\Omega}_{xt}^e} = \sum_{i=1}^{4} \int_{\bar{\Omega}_{xt}^e} \left\{ \frac{\partial E_i^e}{\partial \{\delta^e\}} \right\} \left\{ \frac{\partial E_i^e}{\partial \{\delta^e\}} \right\}^T d\Omega_{xt} \tag{3.69}$$

3.3.3 1D Phase Field Mathematical Model

In the 1D numerical studies we have also shown comparison of the results from the proposed approach to phase field models for which the numerical solutions are also obtained using space-time LSP. We present details in the following.

Considering phase change of an incompressible isotropic material with pure conduction in one dimension. The energy and phase field equations reduce to,

$$\rho c_p \frac{\partial T}{\partial t} - \frac{\partial}{\partial x}\left(k \frac{\partial T}{\partial x}\right) + \frac{1}{2} L_f \frac{\partial p}{\partial t} = 0 \qquad \forall\, x, t \;\in\; \Omega_{x,t} = \Omega_x \times (0, \tau) \tag{3.70}$$

$$\alpha \xi^2 \frac{\partial p}{\partial t} - \xi^2 \frac{\partial^2 p}{\partial x^2} + \frac{\partial f}{\partial p} = 0 \qquad \forall\, x, t \;\in\; \Omega_{x,t} = \Omega_x \times (0, \tau) \tag{3.71}$$

The density, ρ, specific heat, c_p, and thermal conductivity, k, are assumed constant regardless of the phase. The latent heat, L_f, is prescribed a value of 0 for the solid phase and a value of 1 for the liquid phase. The phase field variable, p, requires additional constants α and ξ, which are defined as the relaxation time and a parameter that controls the interface thickness, and thus the sharpness of the phase front. In the numerical studies, the free energy density, $f(p, T)$, is defined as,

$$f(p, T) = \frac{1}{8a}(p^2 - 1)^2 - \frac{\xi \Delta s}{3\sigma} T \phi(p)$$

where a is a constant that controls the maximum of the double-well potential, Δs is the change in entropy between the two phases, and σ is the interface surface tension defined

as $\sigma = \frac{2\xi}{3\sqrt{a}}$. The weight function, $\phi(p)$, has the following requirements based on the conclusions of Almgren [27]:

- $\phi(p)$ is an odd function of p
- $\phi(\pm 1) = \pm 1$
- $\phi'(\pm 1) = 0$.

For numerical simulations presented, $\phi(p) = \frac{1}{2}p\left(3 - p^2\right)$. Taking the derivative of the free energy density with respect to p gives,

$$\frac{\partial f}{\partial p} = \frac{p}{2a}\left(p^2 - 1\right) - \frac{3\Delta s\sqrt{a}}{4}T\left(1 - p^2\right) \tag{3.72}$$

Substituting (3.72) into (3.71), the following is obtained:

$$\begin{aligned} &\alpha\xi^2\frac{\partial p}{\partial t} - \xi^2\frac{\partial^2 p}{\partial x^2} + \frac{p}{2a}\left(p^2 - 1\right) - \frac{3\Delta s\sqrt{a}}{4}T\left(1 - p^2\right) = 0 \\ &\forall\, x, t \;\in\; \Omega_{x,t} = (0,1) \times (0,\tau) \end{aligned} \tag{3.73}$$

Equations (3.70) and (3.73) complete the mathematical model for phase change using the phase field approach in one-dimension. These can also be recast as a system of first order PDEs using auxiliary equations.

$$r = \frac{\partial p}{\partial x} \tag{3.74}$$

$$s = k\frac{\partial T}{\partial x} \tag{3.75}$$

Substituting (3.74) and (3.75) into (3.70) and (3.72),

$$\rho c_p\frac{\partial T}{\partial t} - \frac{\partial s}{\partial x} + \frac{1}{2}L_f\frac{\partial p}{\partial t} = 0 \tag{3.76}$$

$$\alpha\xi^2\frac{\partial p}{\partial t} - \xi^2\frac{\partial r}{\partial x} + \frac{p}{2a}\left(p^2 - 1\right) - \frac{3\Delta s\sqrt{a}}{4}T\left(1 - p^2\right) = 0 \tag{3.77}$$

$$r - \frac{\partial p}{\partial x} = 0 \tag{3.78}$$

$$s - \frac{\partial T}{\partial x} = 0 \tag{3.79}$$

In this model T, p, r, and s are dependent variables. Details of the space-time LSP are exactly parallel to the 1D case with first order system of PDEs presented in section 3.3.1 case (b) and hence are omitted.

Chapter 4

Numerical Studies

4.1 Introduction

In this chapter we consider 1D and 2D phase change model problems that are commonly used in the published work. The purpose of these numerical studies is multi-fold. From the material presented in Chapters 1 and 2 it is clear that the sharp interface method and the phase field method of describing liquid-solid phase phenomena lead to mathematical models that have their own limitations and merits (see Chapter 2). A significant shortcoming of these methods is that they require a priori existence of a liquid-solid interface at the commencement of the evolution. Secondly, a theoretical solution using the sharp interface 1D model is only possible when c_p and k are constant. In the phase field approach, a priori knowledge of the free energy density and the existence of the interface at the commencement of the solution are essential. Thus the selection of this 1D model problem is done in such a way that the computed evolution from the present approach can be compared with sharp interface and phase field methods. Additional 1D phase change problems are chosen

and are simulated to demonstrate the capability of the present method to initiate a smooth front and propagate it during evolution with changing c_p, k and L_f between the two phases. 2D model problems demonstrate the same features of the proposed approach as in the case of 1D i.e.initiation of a front, variable c_p, k and L_f between the two phases and accurate propagation of the front in two dimensional domains in which the interface zone separating the two phases can be complex.

4.2 Choice of Model Problems and Description of Computational Procedure

The selection of the model problems and the numerical studies presented in this chapter are summarized in this section. Details of the computational procedure are also summarized. The model problems for numerical studies are described in the following.

(1) In this group we consider a 1D model problem (Model Problem 1) with constant c_p and k in which the liquid-solid interface is prescribed in the initial condition. For this model problem, the sharp interface method using the integral form of the mathematical model provides a theoretical solution (Chapter 2). This model problem can also be simulated using the phase field method. The main purpose of this model problem is to compare our computed results (smooth interface method) with the sharp interface theoretical solution and with the phase field model simulation using space-time LSP in ***h,p,k*** framework. Location of the front, temperature distribution, and front propagation during evolution are compared using all three approaches.

(2) The second group of numerical simulations (Model Problem 2) use 1D model prob-

lems also in which the capability of the smooth interface method proposed here to simulate the initiation of the liquid-solid or solid-liquid interface and its subsequent propagation during evolution is demonstrated. The specific heat c_p, thermal conductivity k and latent heat of fusion L_f vary in a continuous and differentiable manner from liquid to solid phases and vice-versa (as described in Chapter 2). One model problem considers the initial phase to be liquid whereas the other model problem the initial phase is considered to be solid to demonstrate the effectiveness of the smooth interface approach in simulating the initiation of the front and its properties in either freezing or melting. These model problems can not be simulated using sharp interface or phase field methods due to the fact that: (a) they require capability to initiate a front (b) and secondly due to variations in c_p, k and L_f in the transition zone both of which are lacking in these two methods.

(3) In the third group of numerical studies we consider two model problems with two dimensional square spatial domains.

   (a) The first model problem (Model Problem 3) considers the initial phase to be liquid with constant temperature BCs on two opposing faces and parabolic heat flux (cooling) on the remaining two opposing faces to demonstrate the initiation of the liquid-solid front in a freezing process in a 2D spatial domain and its propagation during the evolution.

   (b) The second model problem (Model Problem 4) considers the initial phase to be solid with uniform heat flux (heating) on all four boundaries. This model problem demonstrates initiation of a rather complex liquid-solid front that propagates inward from the edges of the square during evolution.

All numerical studies are performed using space-time least squares finite element processes for a space-time strip (in 1D cases) or a space-time slab (in 2D cases) with time marching. The mathematical models utilized in the computational studies are a system of first order PDEs derived using auxiliary variables and auxiliary equations (described in Chapter 2). In case of 1D, the space-time domain of a space-time strip for an increment of time is discretized using nine-node p-version space-time elements. For 2D spatial domains resulting in a space-time slab, the space-time domain is discretized using 27-node p-version space-time elements. The local approximation in both 1D and 2D cases consist of class C^0 in space as well as in time.

For an increment of time i.e. for a space-time strip or a slab, solution of the non-linear algebraic systems is obtained using Newton's linear method with line search. Newton's linear method is considered converged when the absolute value of each component of $\delta I = \{g\}$ is below a preset threshold Δ, numerically computed zero. $\Delta < 10^{-6}$ has been used in all numerical studies. Discretization and p-levels (considered to be uniform in space and time) are chosen such that the least squares functional I resulting from the residuals for the entire space-time strip or slab is always of order of $O(10^{-6})$ or lower and hence good accuracy of the evolution is always ensured.

4.3 Model Problem 1: 1D Phase Change with Comparisons to Sharp Interface and Phase Field Solutions

This 1D model problem is chosen such that the numerical solution computed using the present approach (smooth interface) can be compared with the theoretical solution from the sharp interface method and the numerically computed solution from the phase field method. Figure 4.1 shows a schematic of the first space-time strip for an increment of time Δt and boundary conditions at $x = 0$ and $x = 1$ of a spatial domain of unit length. Figure 4.1 also shows details of the spatial discretization. The initial conditions at time $t = 0$ consist of prescribed temperature distribution obtained from the sharp interface theoretical solution. $x = 0.14$ marks the location of the interface. For $0 \leq x \leq 0.14$ the domain is solid whereas for $0.14 \leq x \leq 1$ the domain is liquid.

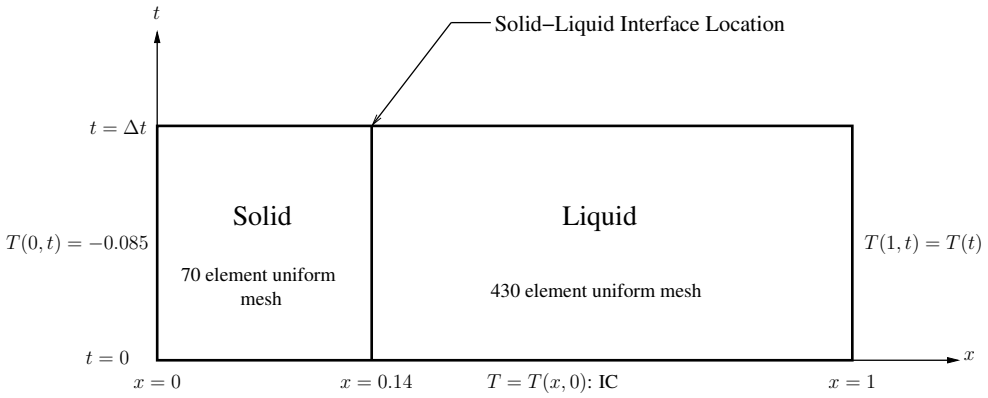

Figure 4.1: Schematic of the First Space-Time Strip, BCs, IC and Spatial Discretization

$$T(1,t) = -0.015 \frac{\text{erf}\left(\frac{\beta}{2}\right) - \text{erf}\left(\frac{1}{2\sqrt{t+t_0}}\right)}{1 - \text{erf}\left(\frac{\beta}{2}\right)}$$

Figure 4.2 shows the temperature field as a function of x-coordinate prescribed as the initial condition at $t = 0$. The solid phase is discretized using a 70 element uniform mesh of nine node p-version hierarchical space-time elements. The liquid phase is discretized using a 430 element uniform mesh of the same type of space-time elements. We describe details of the phase field numerical solution and smooth interface numerical solution in the following sections.

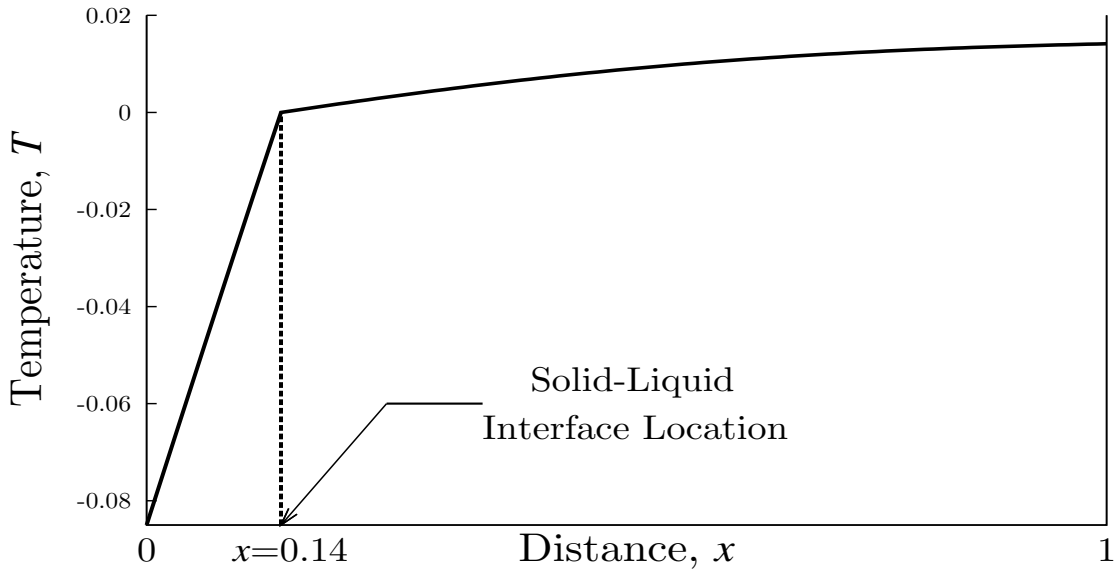

Figure 4.2: Initial Condition at $t = 0$, Temperature Distribution from the Theoretical Solution Using Sharp Interface Model

Phase Field Solution:

The computations of the evolution using the phase field model are done using space-time LSP based on a system of first order PDEs (see Chapters 2 and 3) with local approximations of class C^0 in space and time. We consider the following properties and parameters.

$$\rho = 1,\ \alpha = 1,\ \Delta s = 1,\ a = 1, \text{ and } \xi = 0.008$$

Evolution was computed using 1000 time steps and a p-level of 4 in space and time with $\Delta t = 0.001$. For all space-time strips I values of the order of $O(10^{-8})$ or lower were obtained. The maximum values of the $|g_i|_{max}$ were of the order of $O(10^{-6})$ or lower. The convergence of the Newton's linear method with line search required iterations that range between 5-10 for the entire range of 1000 time increments.

Smooth Interface Solution (Present Approach):

c_p and k were held constant as required by the sharp interface theoretical solution. We consider the following properties and parameters,

$$\rho = 1, T_s = -0.001, T_m = 0.0, T_l = 0.001$$

$$c_{ps} = c_{pl} = 1, k_s = k_l = 1, L_f = 1$$

Thus, with these choices the width of the interface zone is 0.002 units in temperature centered at $T_m = 0.0$. Figure 4.3 shows a schematic of the smooth interface in the spatial domain. The temperature distribution $[T_s, 0]$ occurs over less than one element whereas $[0, T_l]$ is over 18 elements.

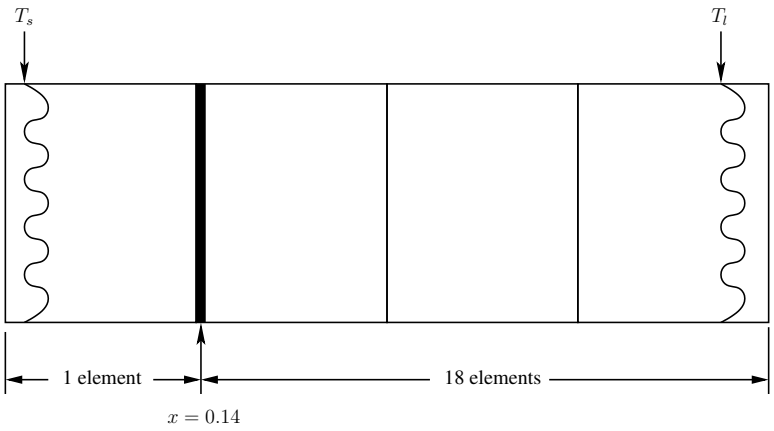

Figure 4.3: Schematic of Initial Smooth Interface over Spatial Discretization: Model Problem 1

Evolution is computed for 100 increments of time with $\Delta t = 0.01$ with p-level of 3 in both space and time. The convergence of the Newton's method with line search requires between 5 - 10 iterations for the entire range of 100 time increments. The maximum values of $|g_i|_{max}$ were of the order of $O(10^{-6})$ or lower for the entire evolution. The I values are of the order of $O(10^{-7})$ or lower during the entire evolution. The latent heat L_f is expressed as a polynomial in temperature in the interface zone.

$$L_f(T) = c_0 + \sum_{i=1}^{n} c_i T^i \qquad ; T_s \leq T \leq T_l$$

Generally $n = 3$ (a cubic polynomial in temperature) or $n = 5$ (a fifth order polynomial in temperature) is found adequate. The coefficient c_0 and c_i are calculated using the conditions at $T = T_s$ and $T = T_l$.

For $n = 3$

at $T = T_s$: $L_f(T) = 0, \quad \frac{dL_f(T)}{dT} = 0$

at $T = T_l$: $L_f(T) = L_f, \quad \frac{dL_f(T)}{dT} = 0$

For $n = 5$

at $T = T_s$: $L_f(T) = 0, \quad \frac{dL_f(T)}{dT} = \frac{d^2L_f(T)}{dT^2} = 0$

at $T = T_l$: $L_f(T) = L_f, \quad \frac{dL_f(T)}{dT} = \frac{d^2L_f(T)}{dT^2} = 0$

Numerical Studies:

We present and discuss numerical solutions from smooth interface and phase field methods and their comparisons with sharp interface theoretical solution in this section. First we consider smooth interface solutions and comparisons with sharp interface theoretical solution. Figure 4.4 shows evolutions of L_f for the first five time steps. Minor oscillations in the evolution are due to the non-differentiable nature of the IC at $x = 0.14$ (location of the front).

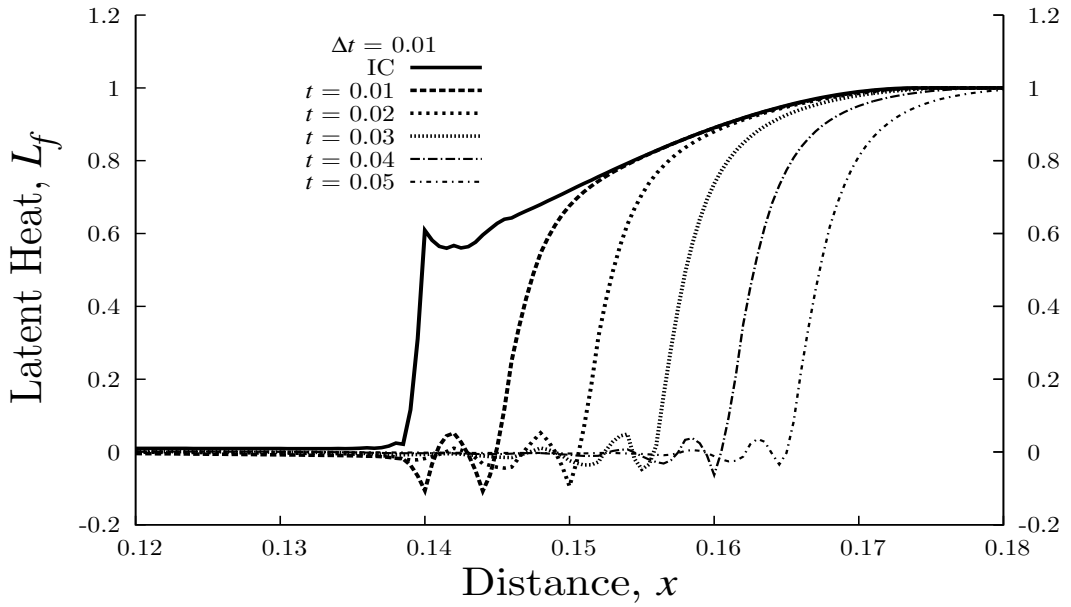

Figure 4.4: Evolution of Latent Heat (Smooth Interface), first 5 time steps: Model Problem 1

As the evolution proceeds (Figure 4.5), the oscillations in the evolution of L_f over the spatial domain diminish and eventually disappear. Figure 4.6 shows evolution of temperature over the spatial domain and a comparison with the theoretical solution from the sharp interface method. Location of the liquid-solid front is marked by the center of the interface region obtained from the smooth interface solution. A comparison with the theoretical solution for $0 \leq t \leq 1$ is presented in Figure 4.7. The agreement between the two is excellent confirming that even extremely hypothetical non-physical conditions used in obtaining the theoretical solution are possible to simulate in the smooth interface approach.

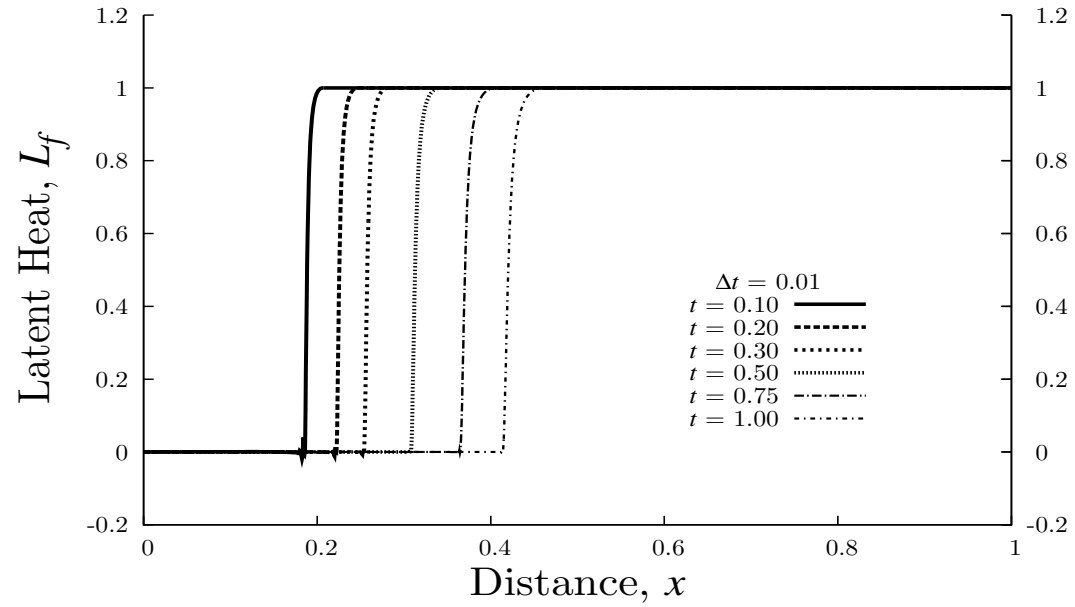

Figure 4.5: Evolution of Latent Heat (Smooth Interface) for $0.1 \leq t \leq 1.0$: Model Problem 1

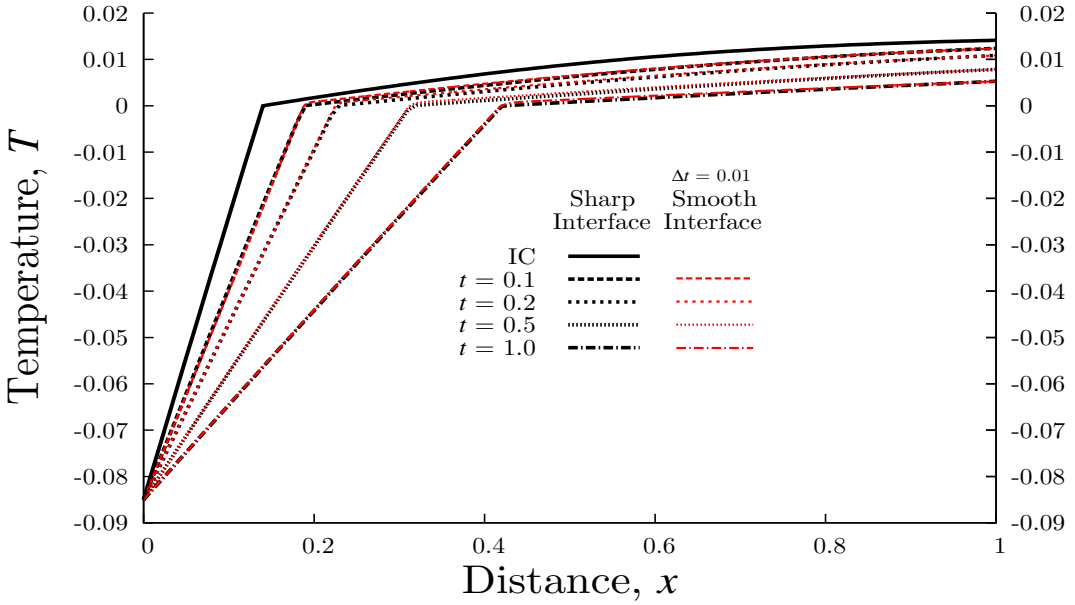

Figure 4.6: Evolution of Temperature using Smooth Interface and Sharp Interface Theoretical Solution: Model Problem 1

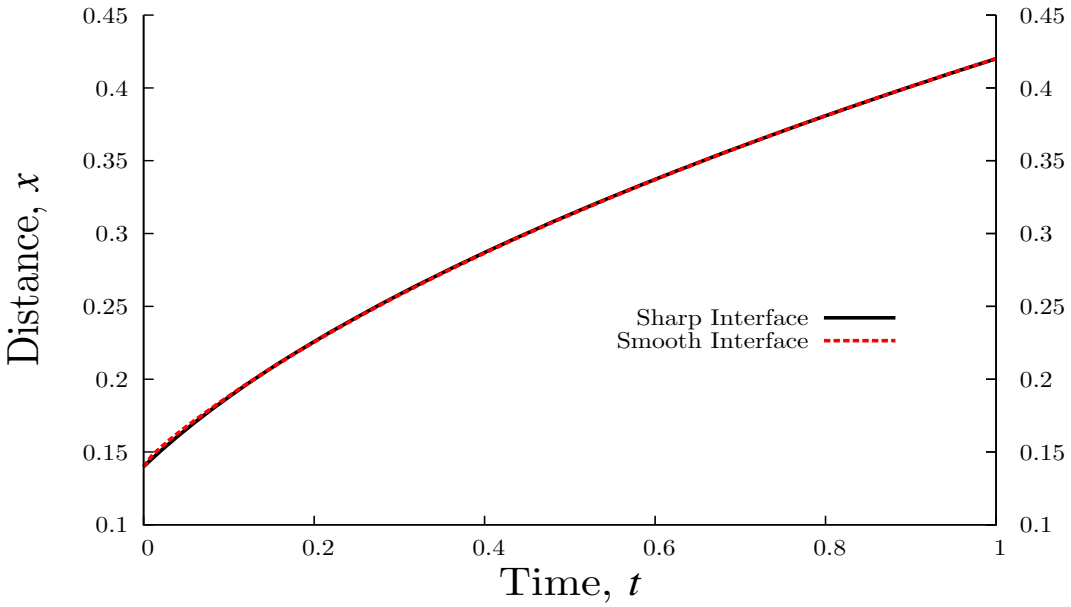

Figure 4.7: Interface Location as a Function of Time: Model Problem 1

Figure 4.8 shows the evolution of the phase field variable p over the spatial domain. Evolution of temperature, location of the front separating liquid-solid phases obtained using phase field method and a comparison with the smooth interface results are shown in Figures 4.9 and 4.10. The agreement is excellent. The numerical studies demonstrate the validity of the smooth interface method as it is able to simulate a standard benchmark 1D problem (even though hypothetical) accurately with excellent agreement with phase field solution and the theoretical solution obtained from the sharp interface method.

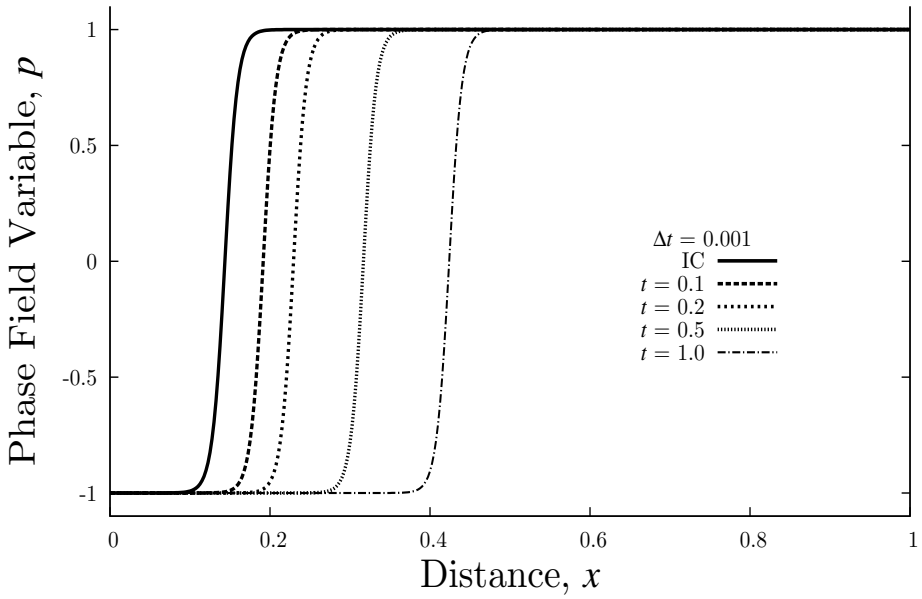

Figure 4.8: Evolution of Phase Field Variable p: Model Problem 1

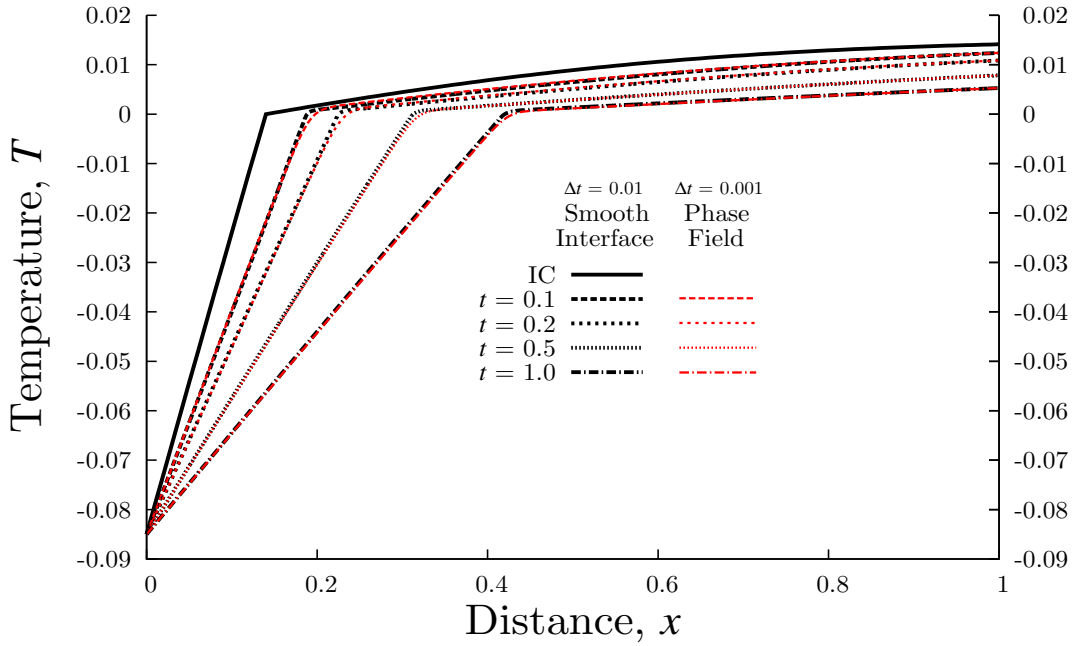

Figure 4.9: Evolution of Temperature using Smooth Interface and Phase Field Solutions: Model Problem 1

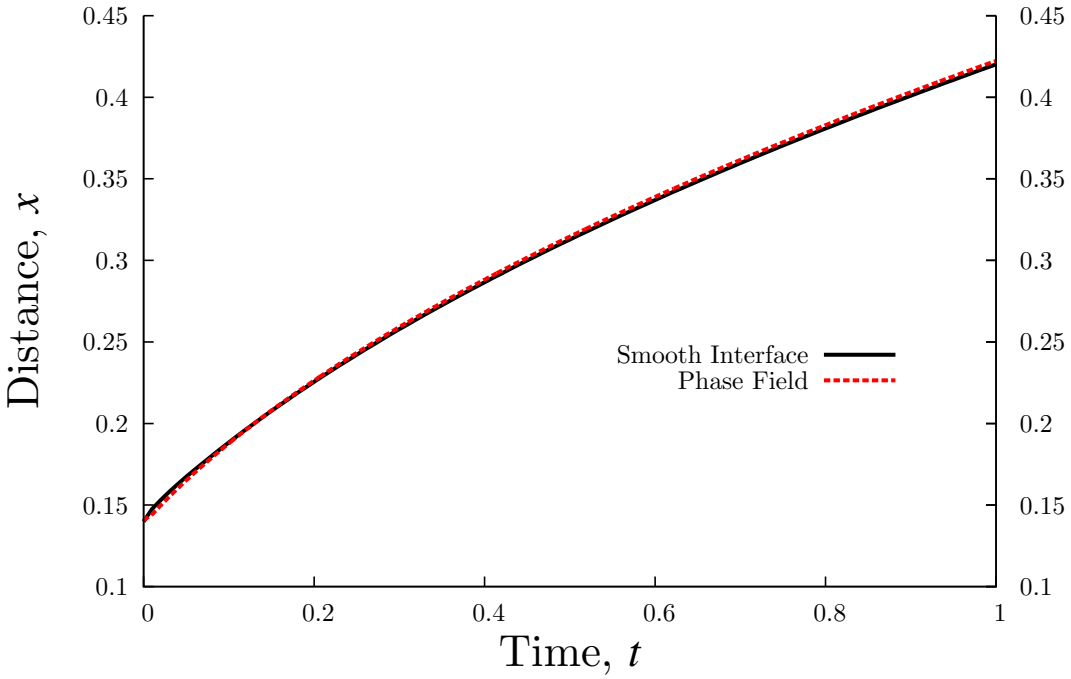

Figure 4.10: Interface Location as a Function of Time: Model Problem 1

4.4 Model Problem 2: 1D Phase Change with Interface Initiation and Propagation; Variable c_p, k, and L_f

In this 1D model problem we consider two cases. In the first case the initial phase at commencement of the evolution is liquid whereas in the second case the initial phase at the commencement of the evolution is solid. In both cases we consider smooth interface method to simulate initiation of the interface and its subsequent propagation during further evolution. In both cases c_p and k have different values in solid and liquid phases with continuous and differentiable distribution in the transition region. Latent heat of fusion L_f is assumed to behave in the same fashion. Details of these distributions have already been

presented in model problem 1.

Case (a): Liquid-Solid Phase Change:

Figure 4.11 shows a schematic of the first space-time strip and BCs at $x = 0$ and at $x = 1$ for a spatial domain of one unit length. At $x = 0$, a constant temperature of $T(0,t) = 0.015$ is maintained while at $x = 1$ a constant heat flux of $q(1,t) = 0.1$ is maintained (heat removal) for all values of time. The initial condition at $t = 0$ consists of constant temperature of $T(x,0) = 0.015$ for the entire spatial domain. We consider the following properties and parameters.

$$\rho = 1, T_s = -0.001, T_m = 0.0, T_l = 0.001$$

$$c_{ps} = 2.1, c_{pl} = 4.2, k_s = 2.0, k_l = 1.0, L_f = 1$$

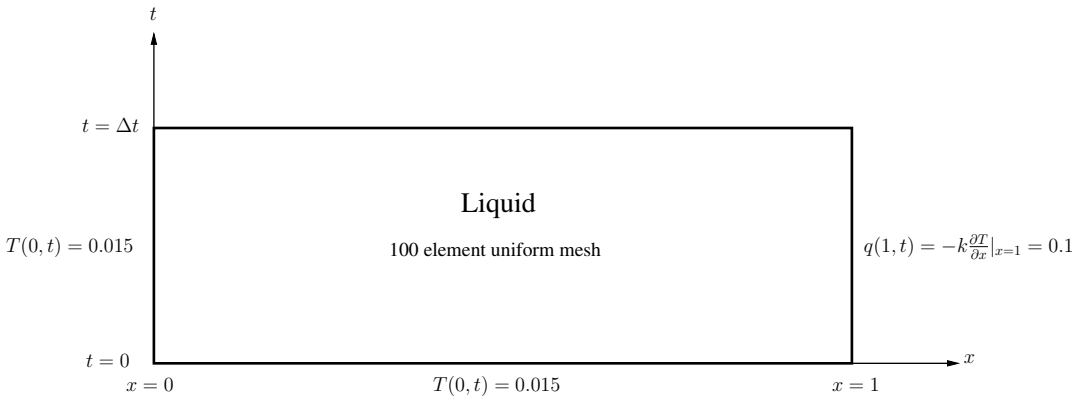

Figure 4.11: Schematic of First Space-Time Strip, BCs, IC and Spatial Discretization

In the interface region $[T_s, T_l]$ we consider the following for c_p, k, and L_f.

$$c_p(T) = c_0 + \sum_{i=1}^{n} c_i T^i$$

$$k(T) = \hat{c}_0 + \sum_{i=1}^{n} \hat{c}_i T^i$$

$$L_f(T) = \tilde{c}_0 + \sum_{i=1}^{n} \tilde{c}_i T^i$$

The coefficients c_0, c_i; $\hat{c}_0$, $\hat{c}_i$ and $\tilde{c}_0$, $\tilde{c}_i$ are evaluated using conditions on $c_p(T)$, $k(T)$, and $L_f(T)$ and their derivatives at $T = T_s$ and $T = T_l$ (see L_f in model problem 1). In the present studies we use $n = 3$. In the numerical studies we consider a p-level of 3 in both space and time with $\Delta t = 0.05$. The Newton's linear method upon convergence yields $|g_i|_{max}$ of the order of $O(10^{-6})$ or lower for the entire evolution consisting of 1000 time increments. The number of iterations range between 5-10 during the computations for all time steps. I values of the order of $O(10^{-7})$ or lower are achieved for all space-time strips. Since the physics of phase-change in this model problem requires initiation of the liquid-solid interface, this model problem can not be simulated using sharp interface or phase field methods. Figures 4.12 and 4.13 show evolution of L_f and T for the first ten time steps. The evolution of L_f and T for $0 \leq t \leq 50$ are shown in Figures 4.14 and 4.15. The evolutions are oscillation free and the sharp fronts are maintained without diffusion during the evolution.

A numerical study with increased width of the interface region is also conducted. In the study we keep all other parameters and properties the same as described above for this model problem, except T_s and T_l are changed to -0.002 and 0.002 which doubles the size of the interface region. Evolutions of latent heat for these values of T_s and T_l as well as $T_s = -0.001$ and $T_l = 0.001$ are shown in Figure 4.16. The center of the interface region marking the front location remains unaffected by increasing the width of the interface region. Figure 4.17 shows the location of the interface for two different choices of T_s and T_l. Excellent agreement confirms that $[T_s, T_l]$ range does not influence the interface location.

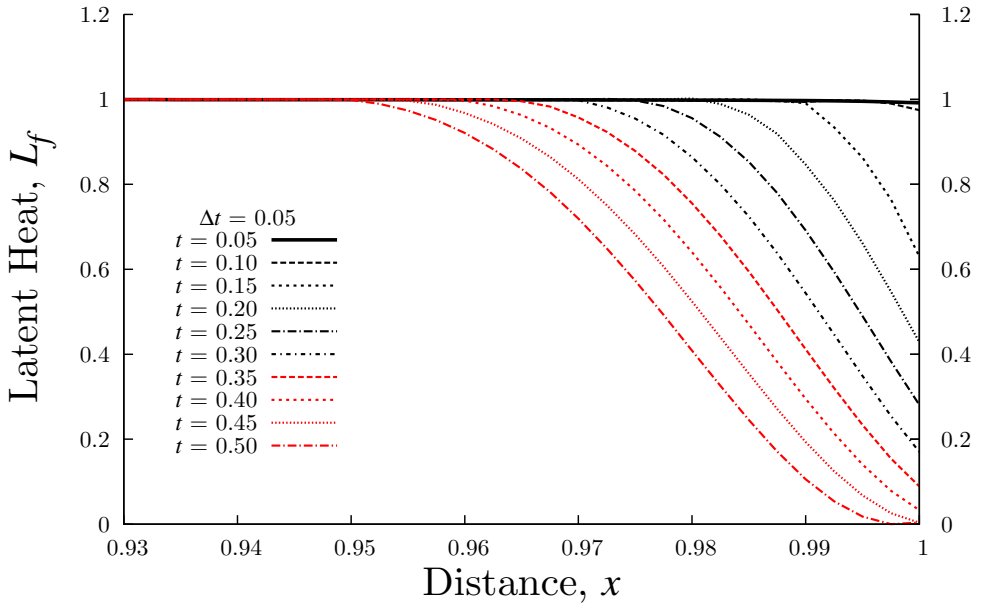

Figure 4.12: Evolution of Latent Heat (Smooth Interface), first 10 time steps: Model Problem 2, Case (a)

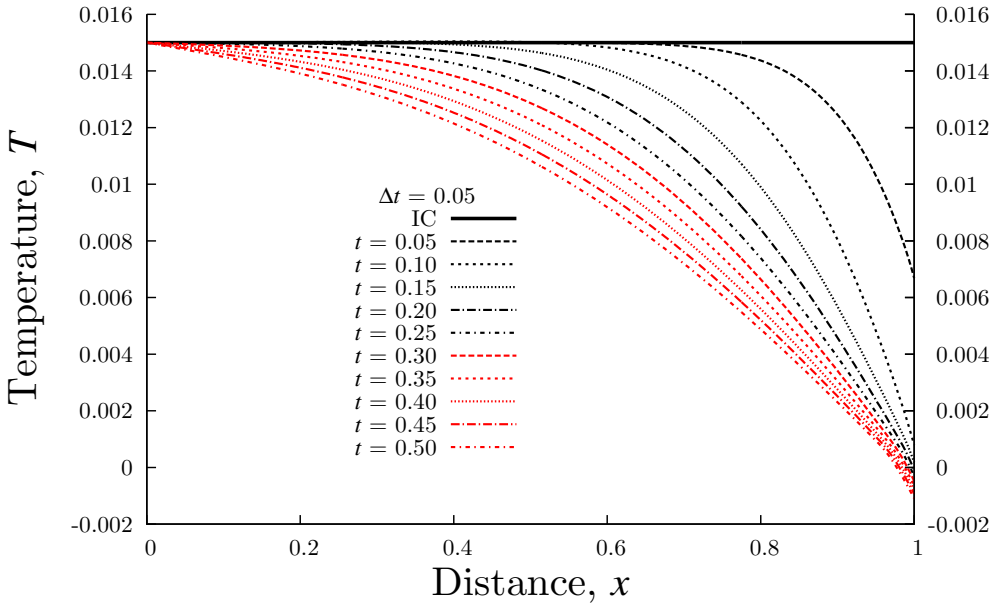

Figure 4.13: Evolution of Temperature (Smooth Interface), first 10 time steps: Model Problem 2, Case (a)

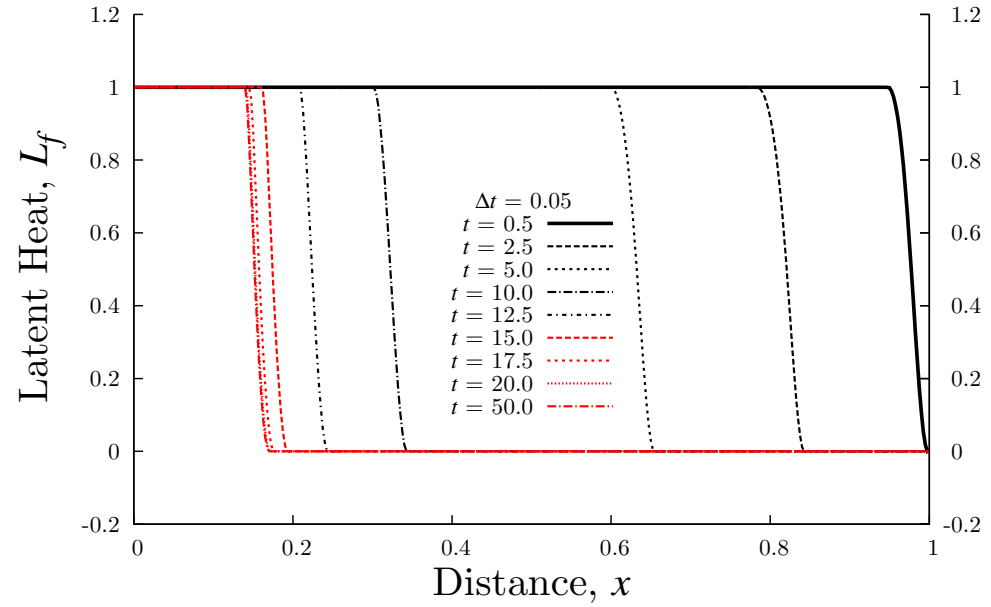

Figure 4.14: Evolution of Latent Heat (Smooth Interface) for $0.5 \leq t \leq 50$: Model Problem 2, Case (a)

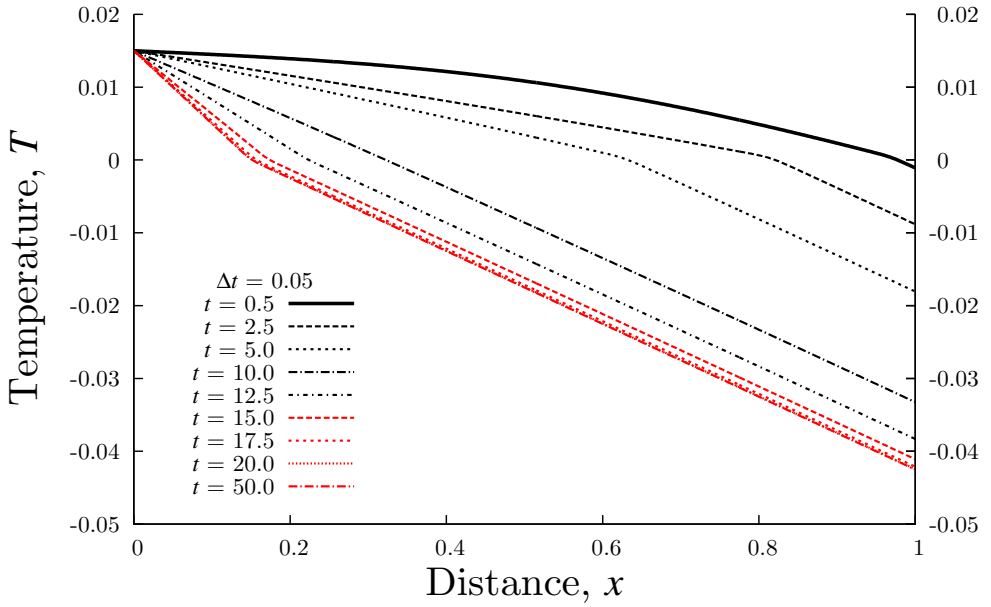

Figure 4.15: Evolution of Temperature (Smooth Interface) for $0.5 \leq t \leq 50$: Model Problem 2, Case (a)

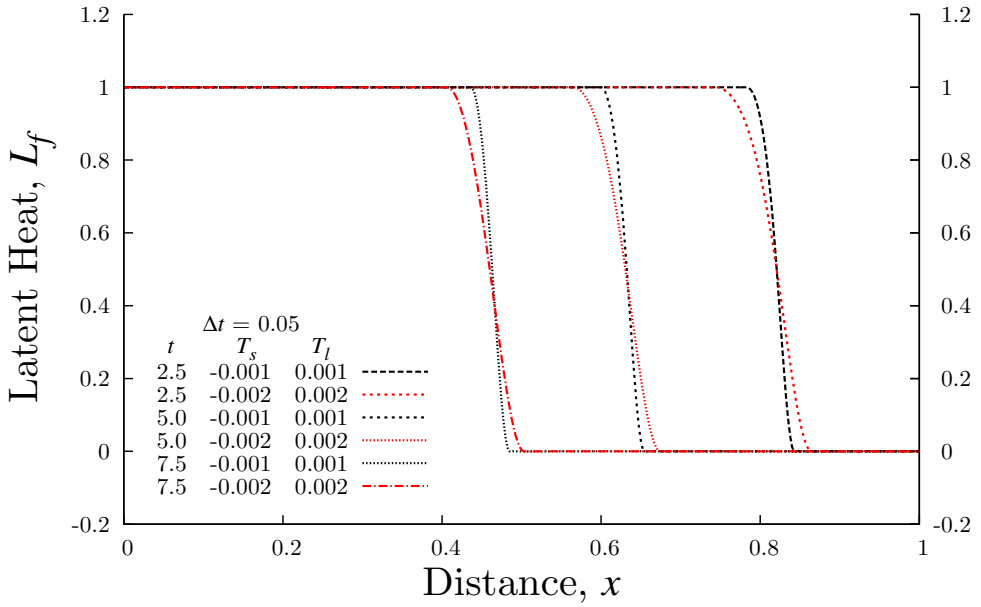

Figure 4.16: Evolution of Latent Heat for Different Temperature Ranges: Model Problem 2, Case (a)

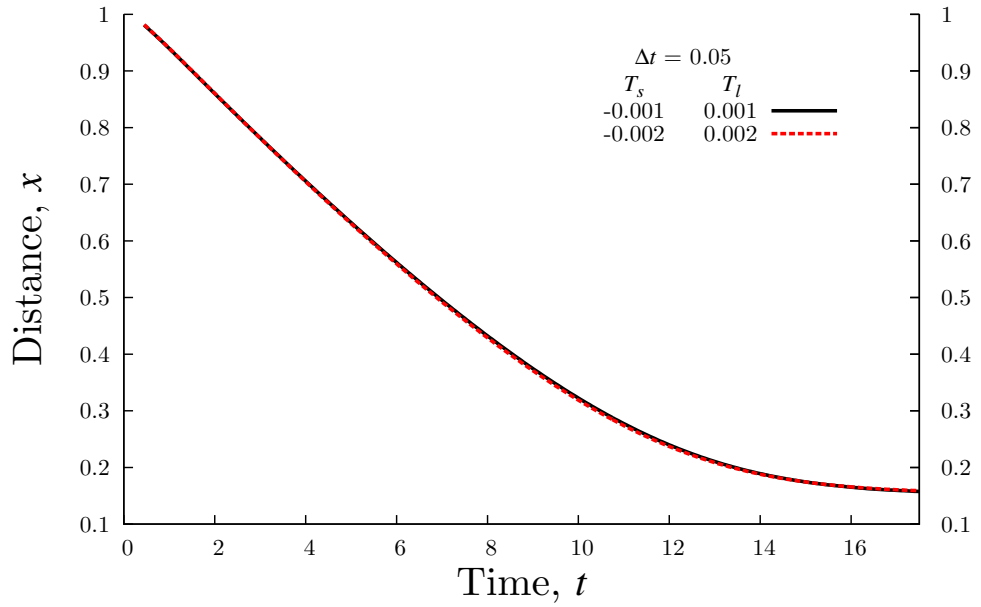

Figure 4.17: Comparison of Interface Location for Different Temperature Ranges: Model Problem 2, Case (a)

Case (b): Liquid-Solid Phase Change:

Figure 4.18 shows the schematic of the first space-time strip and BCs at $x = 0$ consisting of a constant heat flux $q(0,t) = 0.1$ and at $x = 1.0$ a constant temperature of $T(1,t) = -0.015$ for a spatial domain of one unit length. All parameters and properties are the same as for case (a) with $T_s = -0.001$, $T_m = 0.0$, and $T_l = 0.001$ i.e. the transition region of $[-0.001 : 0.001]$ in temperature. The initial condition at $t = 0$ consists of a constant temperature $T(x,0) = -0.015$ i.e. initially the entire spatial domain is solid phase.

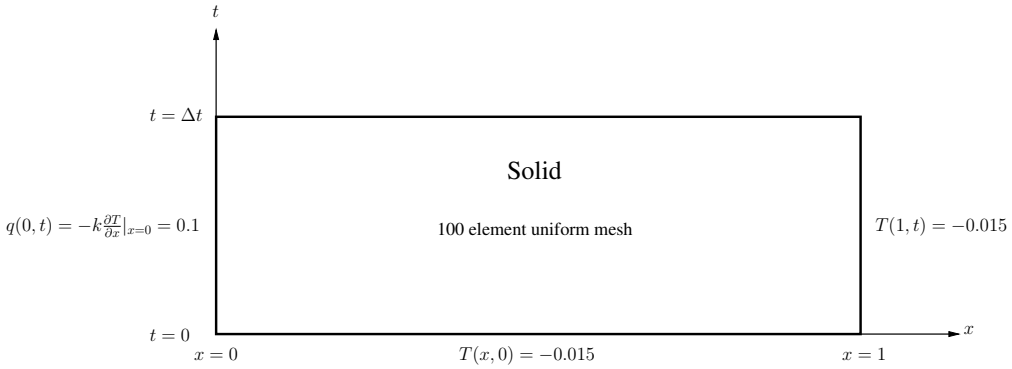

Figure 4.18: Schematic of First Space-Time Strip, BCs, IC and Spatial Discretization

c_p, k, and L_f vary in the transition region in a continuous and differentiable fashion (described in case (a)). Evolution is computed for 1500 time steps using $\Delta t = 0.025$ with p-level of 3 in space and time. I values of the order of $O(10^{-8})$ or lower, $|g_i|_{max}$ values of the order of $O(10^{-6})$ or lower are achieved during the entire evolution. Newton's linear method with line search requires 5-10 iterations for convergence for each increment of time. Figures 4.19 and 4.20 show evolution of L_f and T for the first 15 time increments. Figures 4.21 and 4.22 show the same evolutions for $0.0 \leq t \leq 37.5$. Evolutions are oscillation free, solid-liquid interface is initiated smoothly and propagates without diffusion during the evolution. As in case (a), this model problem can not be simulated using phase field and sharp interface models due to the fact that it requires initiation of the front and

variable c_p, k, and L_f.

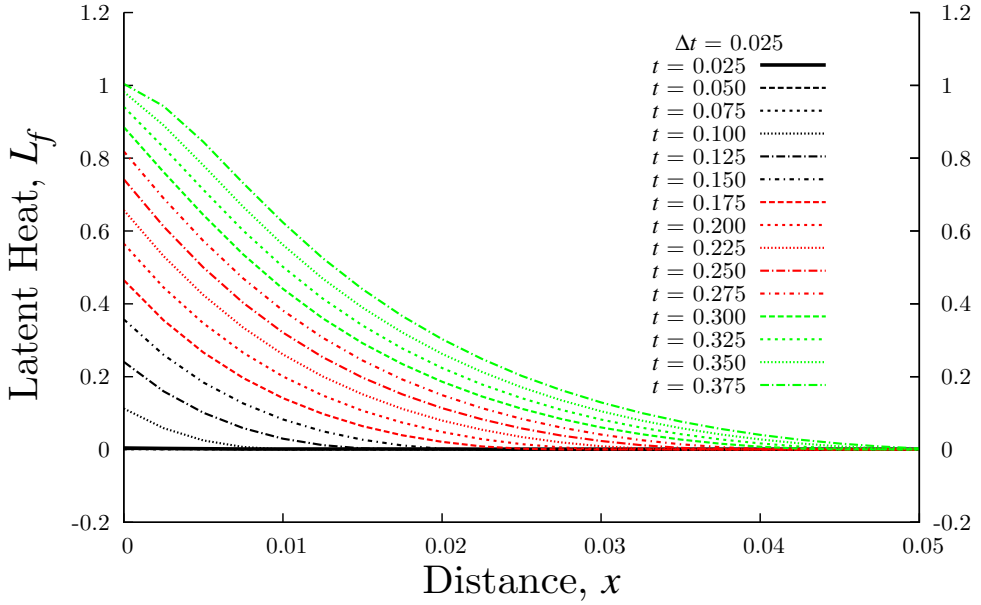

Figure 4.19: Evolution of Latent Heat (Smooth Interface), first 15 time steps: Model Problem 2, Case (b)

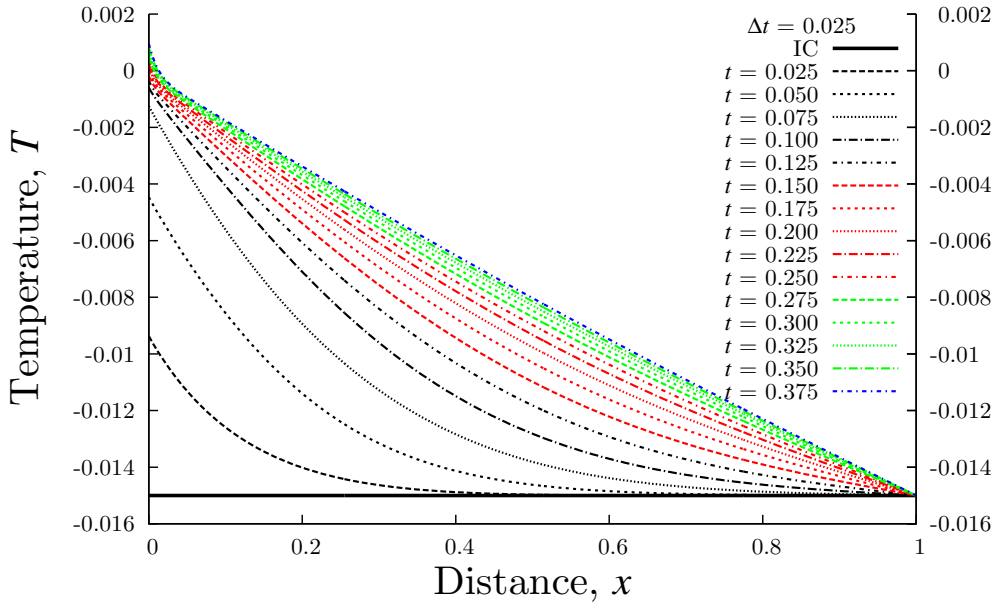

Figure 4.20: Evolution of Temperature (Smooth Interface), first 15 time steps: Model Problem 2, Case (b)

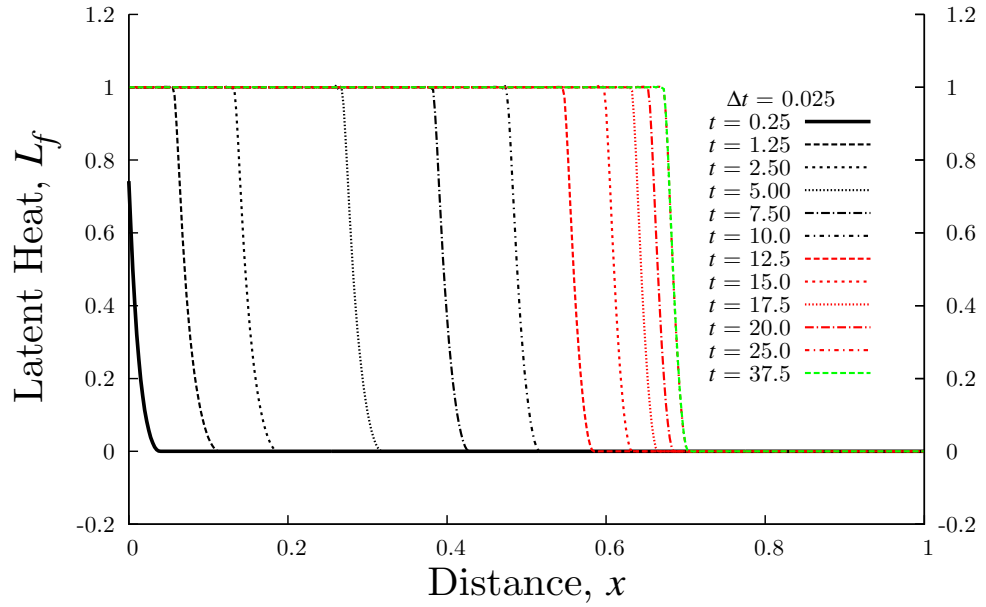

Figure 4.21: Evolution of Latent Heat (Smooth Interface) for $0.25 \leq t \leq 37.5$: Model Problem 2, Case (b)

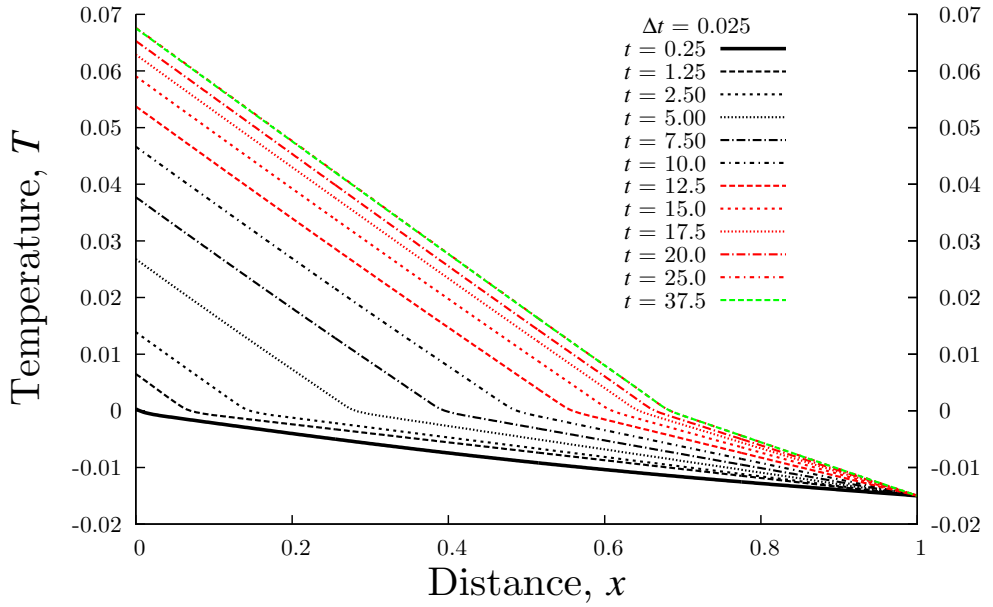

Figure 4.22: Evolution of Temperature (Smooth Interface) for $0.25 \leq t \leq 37.5$: Model Problem 2, Case (b)

4.5 Model Problem 3: 2D Liquid-Solid Phase Change

In this model problem we consider a two dimensional domain consisting of a unit square. A schematic of the domain, boundary conditions and the spatial regions with graded spatial discretizations is shown in Figure 4.23. Table 4.1 provides details of discretization for regions A, B, and C. The boundaries $x = 0$, $0 \leq y \leq 1$ and $x = 1$, $0 \leq y \leq 1$ are maintained at $T = 0.015$ for all values of time. On boundaries $y = 0$, $0 \leq x \leq 1$ and $y = 1$, $0 \leq x \leq 1$ parabolic heat flux is applied (cooling). The following data are used in the numerical studies.

$$\rho = 1, T_s = -0.001, T_m = 0.0, T_l = 0.001$$

$$c_{ps} = 2.1, c_{pl} = 4.2, k_s = 2.0, k_l = 1.0, L_f = 1$$

c_p, k and L_f are continuous and differentiable in T in the transition region $[T_s, T_l]$. A cubic approximation is used (see one dimensional model problems). Evolution is computed for 60 time increments using $\Delta t = 0.05$ with p-level of 2 in space as well as time with C^0 local approximations in space and time for all 1000 27-node 3D space-time elements of the discretization. I values of the order of $O(10^{-7})$ or lower and $|g_i|_{max}$ of the order of $O(10^{-6})$ are achieved for each space-time slab. Newton's method with line search converged between 5-10 iterations for each space-time slab. Figures 4.24 and 4.25 show evolution of latent heat L_f for $0 \leq t \leq 0.4$ and for $0.5 \leq t \leq 3.0$. The evolution of the temperature for $0 \leq t \leq 0.25$ and for $0.5 \leq t \leq 3.0$ are shown in Figures 4.26 and 4.27. Initiation of liquid solid front (Figure 4.24) occurs smoothly and propagates without oscillations (Figures 4.24 and 4.25). Temperature evolution is smooth and free of oscillations. The study demonstrates the strength of the work in simulating moving 2D front without front tracking techniques. This model problem also can not be simulated using phase field and sharp

interface models due to the same reasons as cited in the case of model problem 2. Quarter symmetry of the evolution is quite obvious from the evolutions in Figures 4.24 - 4.27.

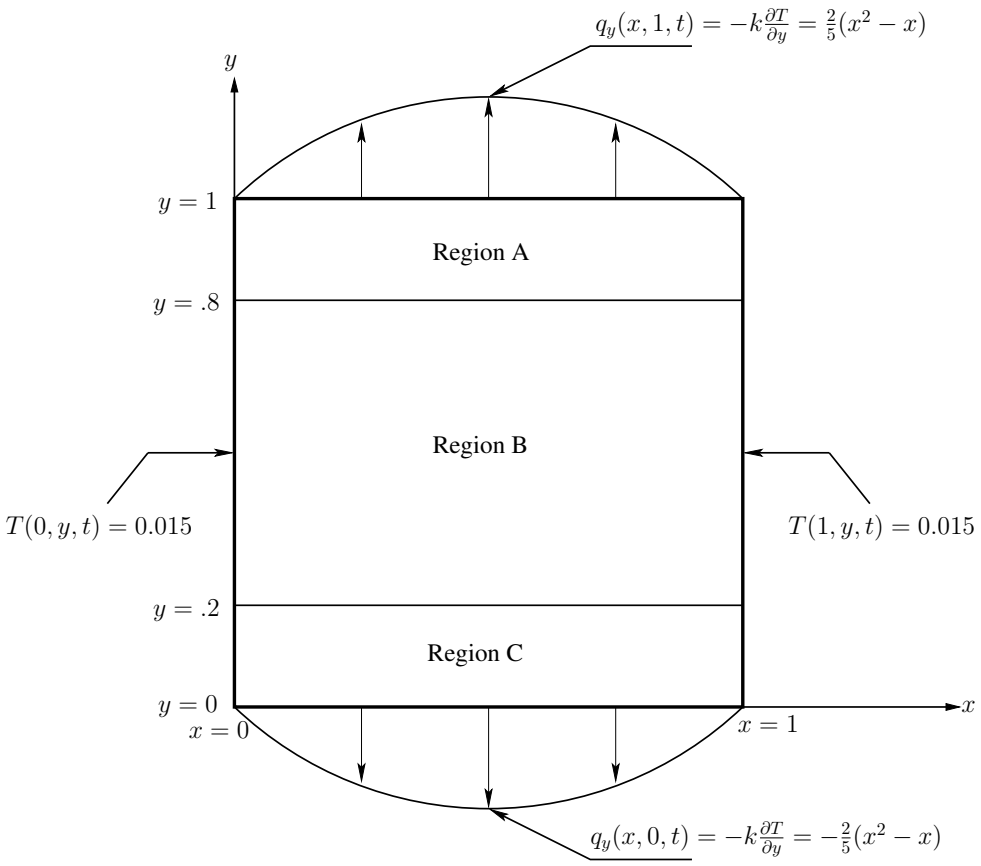

Figure 4.23: Schematic, Discretization and BCs for Model Problem 3

Table 4.1: Spatial Discretization for Model Problem 3

Region	Number of x elements	Number of y elements	h_{ex}	h_{ey}	Number of Total Elements
A	20	20	0.05	0.01	400
B	20	10	0.05	0.06	200
C	20	20	0.05	0.01	400

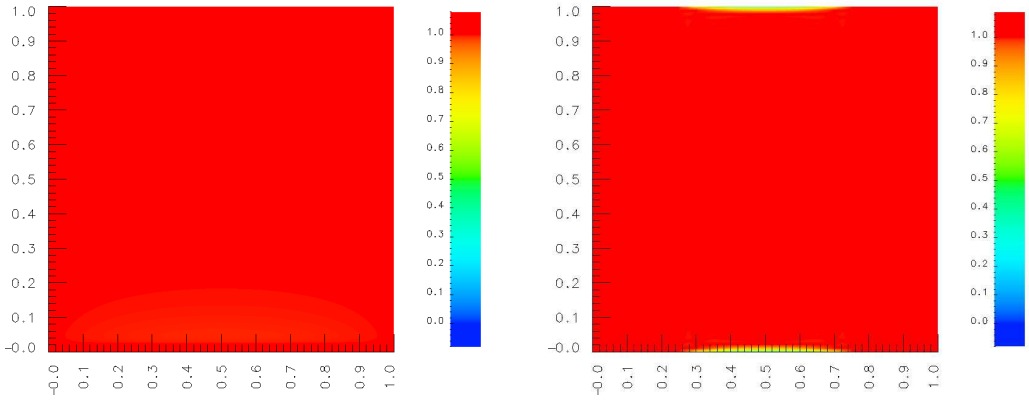

(a) Initial Condition

(b) $t = 0.20$

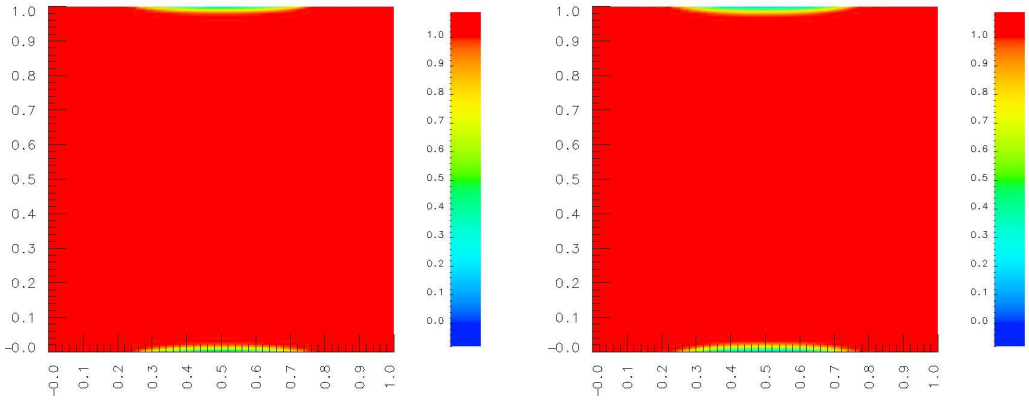

(c) $t = 0.25$

(d) $t = 0.30$

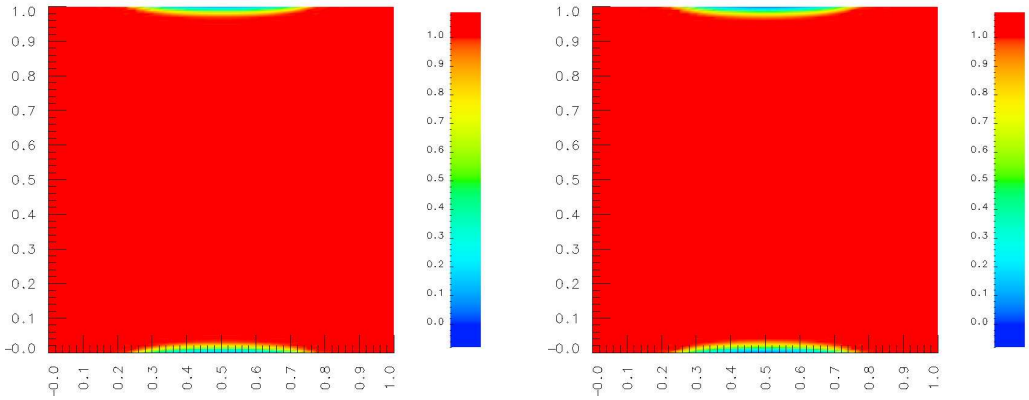

(e) $t = 0.35$

(f) $t = 0.40$

Figure 4.24: Evolution of Latent Heat (Smooth Interface): Model Problem 3, $\Delta t = 0.05$, $0 \leq t \leq 0.40$

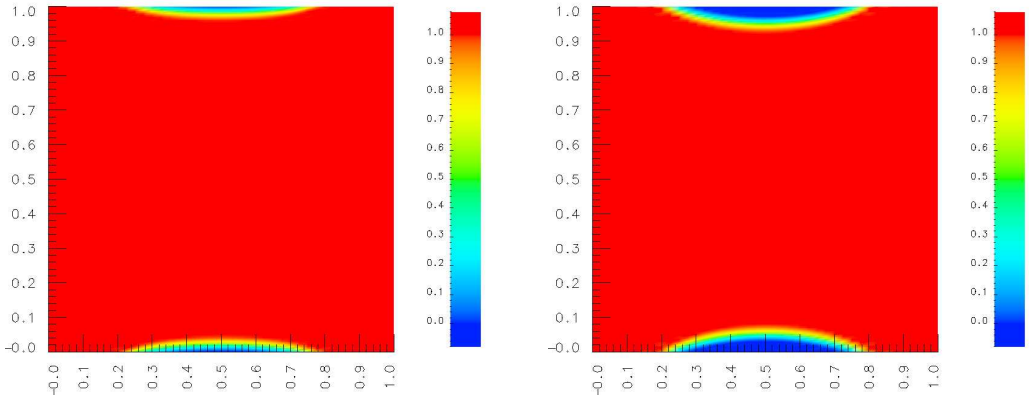

(a) $t = 0.5$ (b) $t = 1.0$

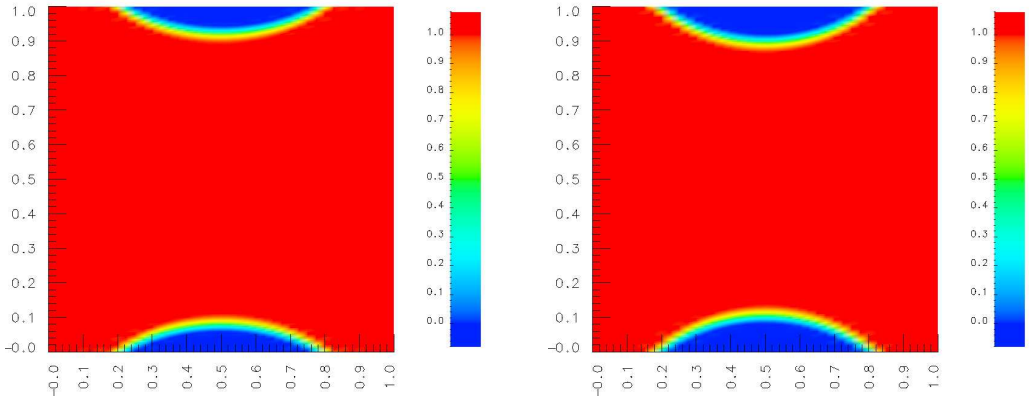

(c) $t = 1.5$ (d) $t = 2.0$

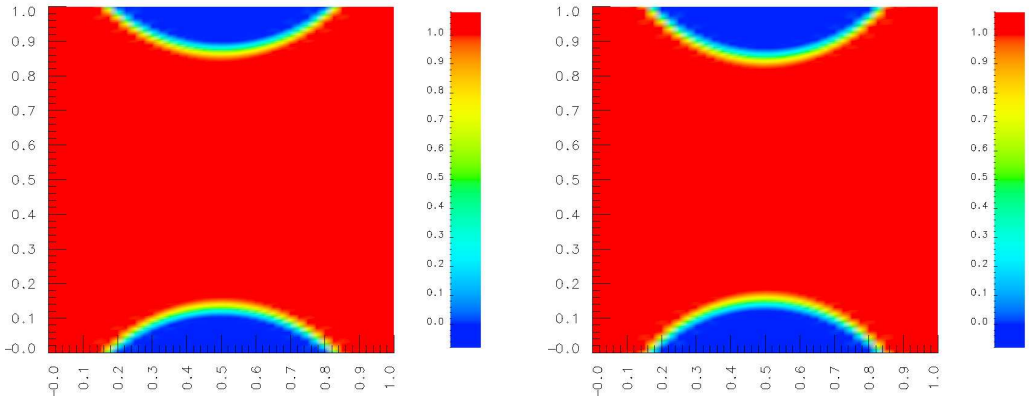

(e) $t = 2.5$ (f) $t = 3.0$

Figure 4.25: Evolution of Latent Heat (Smooth Interface): Model Problem 3, $\Delta t = 0.05$, $0.5 \leq t \leq 3.0$

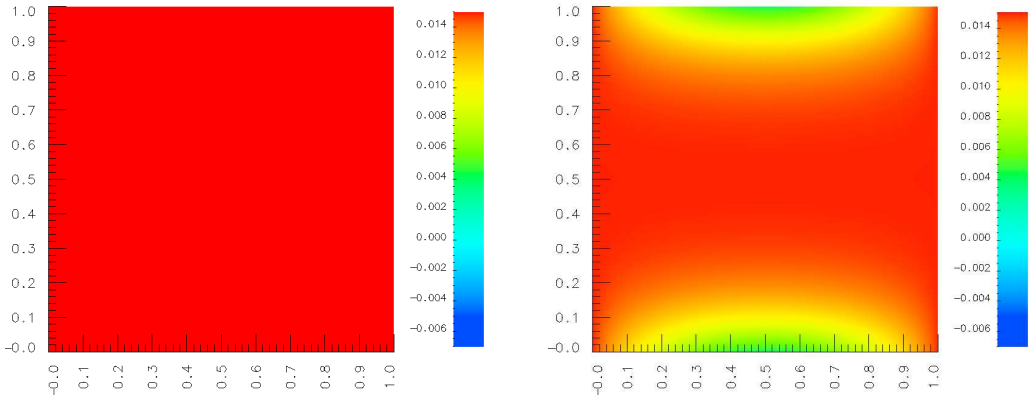

(a) Initial Condition

(b) $t = 0.05$

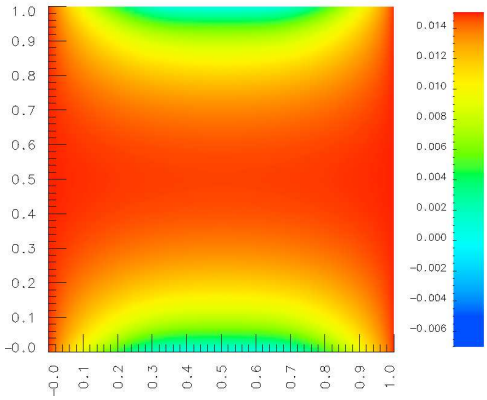

(c) $t = 0.10$

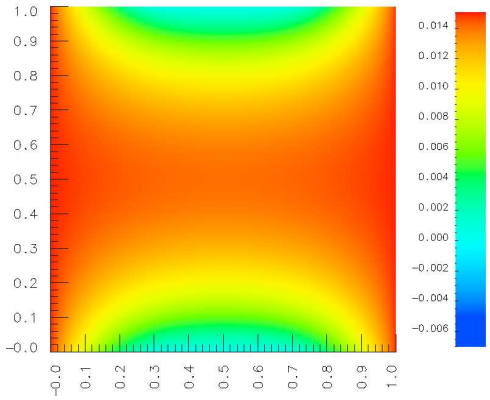

(d) $t = 0.15$

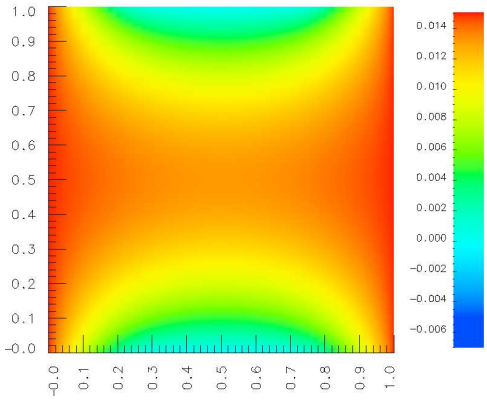

(e) $t = 0.20$

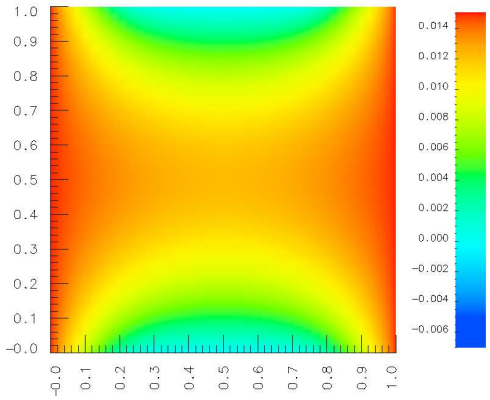

(f) $t = 0.25$

Figure 4.26: Evolution of Temperature (Smooth Interface): Model Problem 3, $\Delta t = 0.05$, $0 \leq t \leq 0.25$

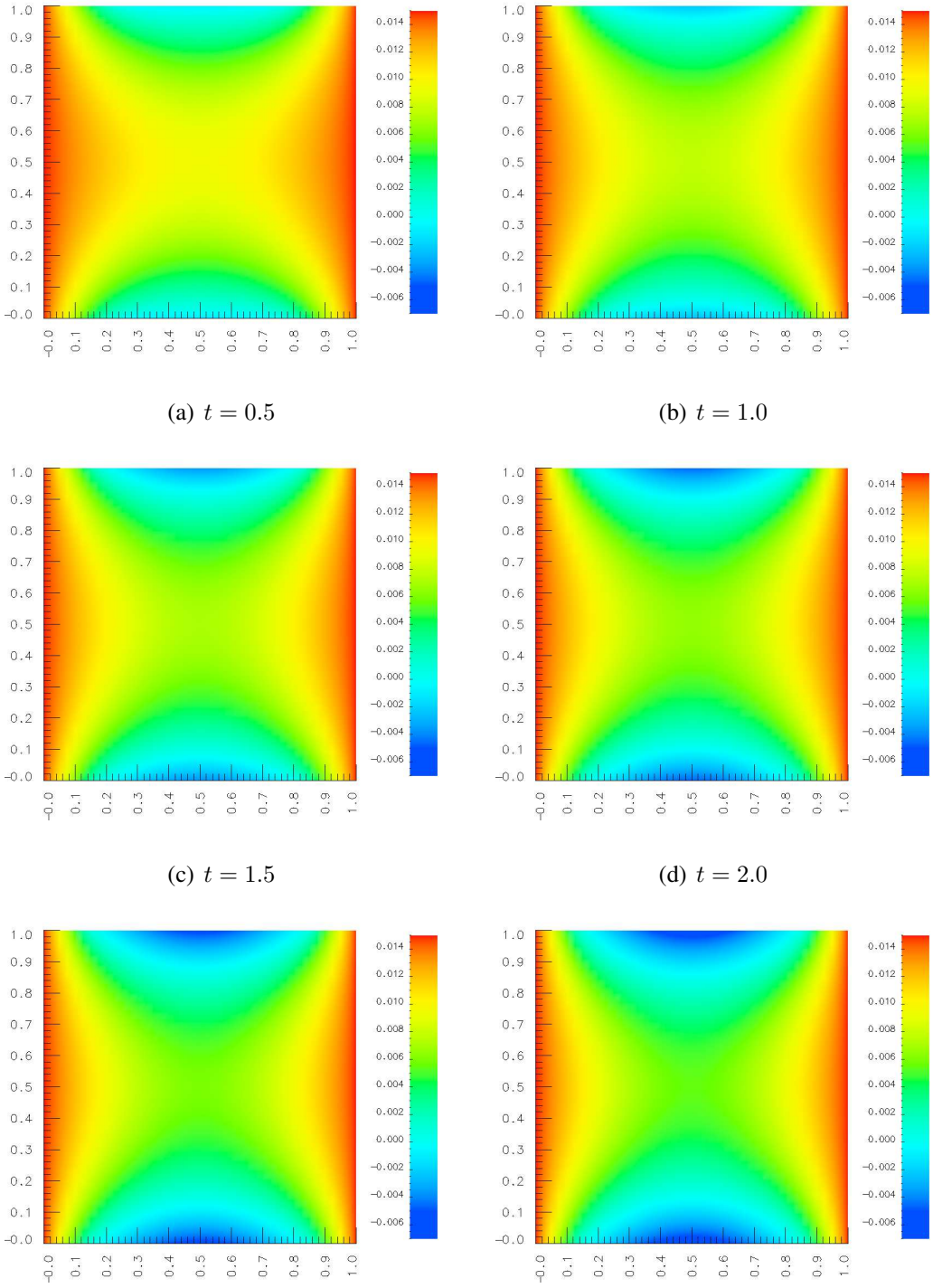

(a) $t = 0.5$ (b) $t = 1.0$

(c) $t = 1.5$ (d) $t = 2.0$

(e) $t = 2.5$ (f) $t = 3.0$

Figure 4.27: Evolution of Temperature (Smooth Interface): Model Problem 3, $\Delta t = 0.05$, $0.5 \leq t \leq 3.0$

4.6 Model Problem 4: 2D Solid-Liquid Phase Change

In this model problem we also consider a two dimensional unit square domain. A schematic of the domain, boundary conditions and the spatial regions marked A-I with graded discretization using 27-node hexahedron space-time elements are shown in Figure 4.28. The details of discretization for each of the regions A-I are given in Table 4.2. All four boundaries of the domain have applied uniform normal heat flux of 0.1 (heat input). The initial condition consists of uniform temperature of -0.015 for the entire spatial domain of the unit square representing solid phase for the entire spatial domain. The data used in the computations of evolution are,

$$\rho = 1, T_s = -0.002, T_m = 0.0, T_l = 0.002$$

$$c_{ps} = 2.1, c_{pl} = 4.2, k_s = 2.0, k_l = 1.0, L_f = 1$$

c_p, k and L_f are assumed to be a cubic function of the temperature in the transition region $[T_s, T_l]$. The evolution is computed for 125 time increments with $\Delta t = 0.01$ and p-level of 2 in space and time with C^0 local approximation in space and time for each element of the space-time slab. I values of the order of $O(10^{-7})$ or lower and $|g_i|_{max}$ values of the order of $O(10^{-6})$ or lower are achieved during the entire evolution. Newton's method with line search converges between 5-10 iterations for each space-time slab during time marching.

Figures 4.29 and 4.30 show evolution of the latent heat for $0 \leq t \leq 0.25$ and for $0.35 \leq t \leq 1.25$. The evolution of the temperature for $0 \leq t \leq 0.05$ and for $0.35 \leq t \leq 1.25$ are shown in Figures 4.31 and 4.32. The solid-liquid interface initiates and propagates smoothly. The entire evolution of L_f and T is smooth and oscillation free. Quarter symmetry of the evolution is quite obvious from Figures 4.29 - 4.32. This model problem has a relatively complex 2D solid-liquid interface or transition region especially

in the vicinity of the corner regions during the initial stages of the evolution. This becomes progressively smoother as the evolution proceeds. This model problem also can not be simulated using phase field or sharp interface methods as it requires initiation of interface and variable c_p, k and L_f.

Table 4.2: Spatial Discretization for Model Problem 4

Region	Number of x elements	Number of y elements	h_{ex}	h_{ey}	Number of Total Elements
A	12	12	0.0167	0.0167	144
B	6	12	0.1000	0.0167	72
C	12	12	0.0167	0.0167	144
D	12	6	0.0167	0.1000	72
E	6	6	0.1000	0.1000	36
F	12	6	0.0167	0.1000	72
G	12	12	0.0167	0.0167	144
H	6	12	0.1000	0.0167	72
I	12	12	0.0167	0.0167	144

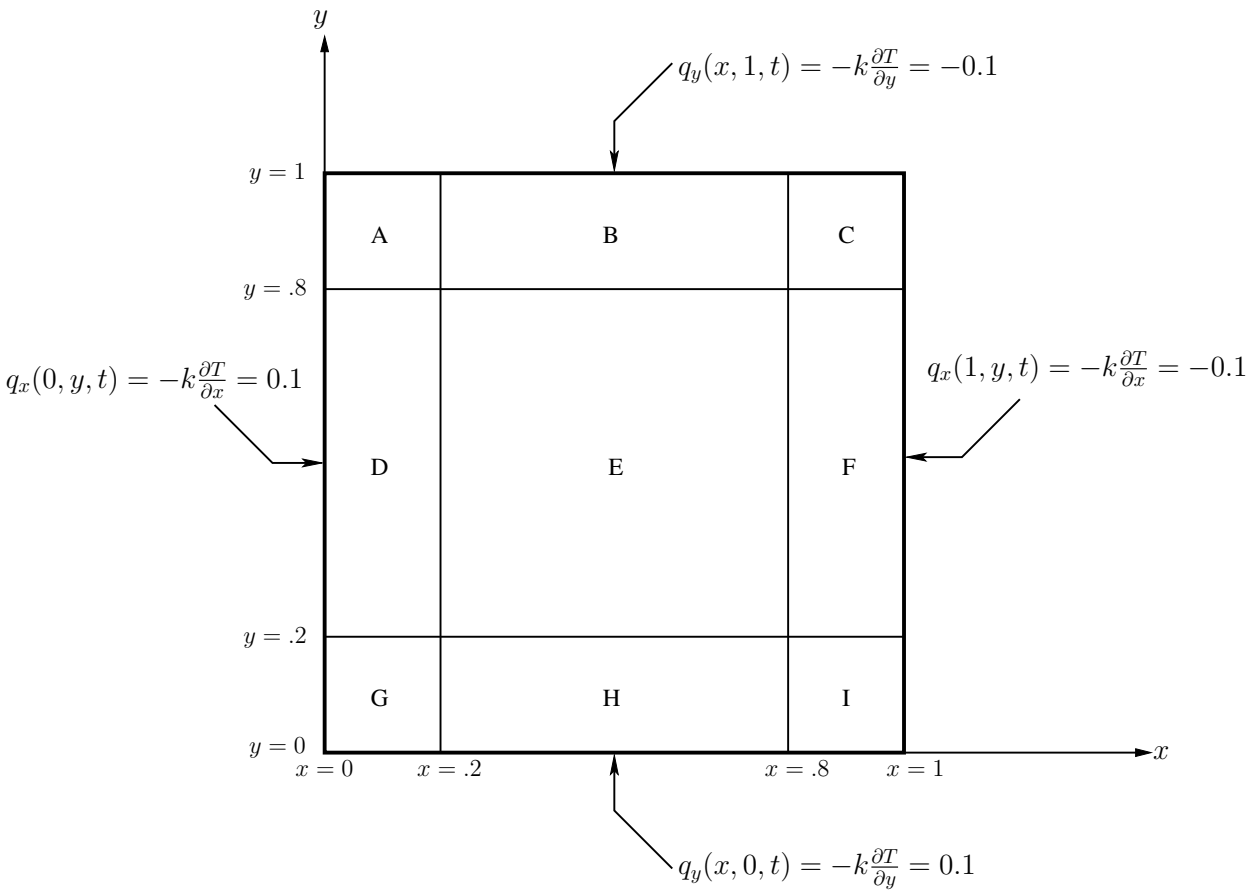

Figure 4.28: Schematic, Discretization and BCs for Model Problem 4

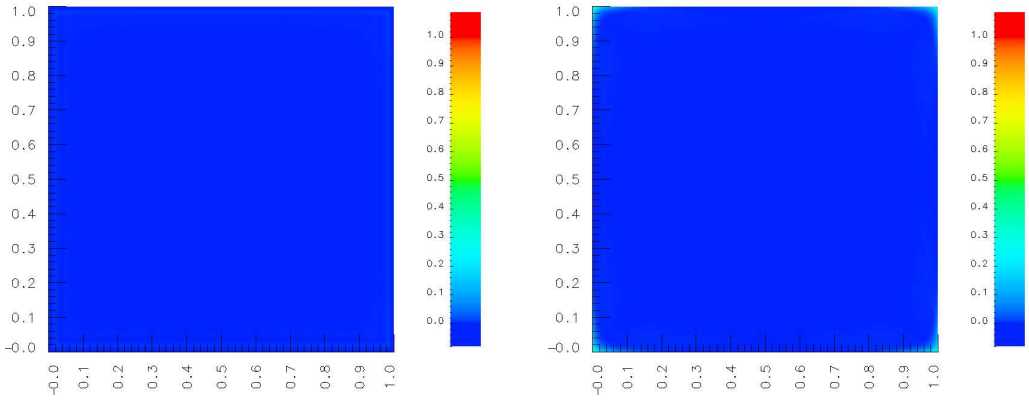

(a) Initial Condition

(b) $t = 0.05$

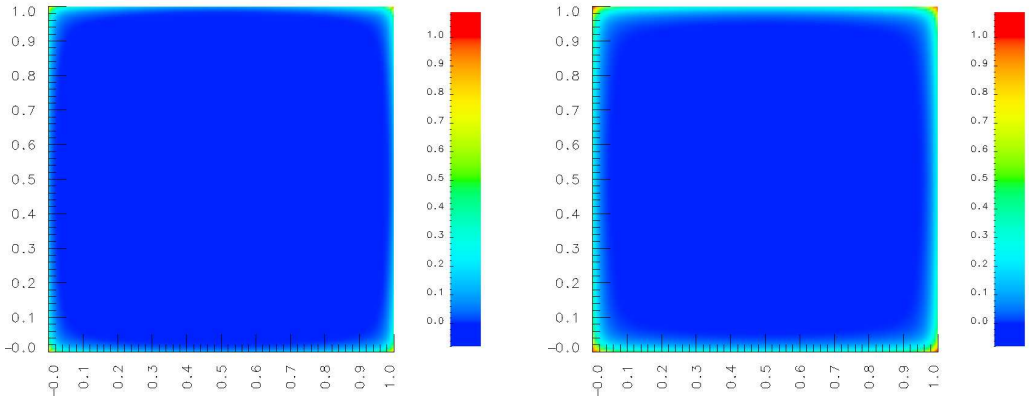

(c) $t = 0.10$

(d) $t = 0.15$

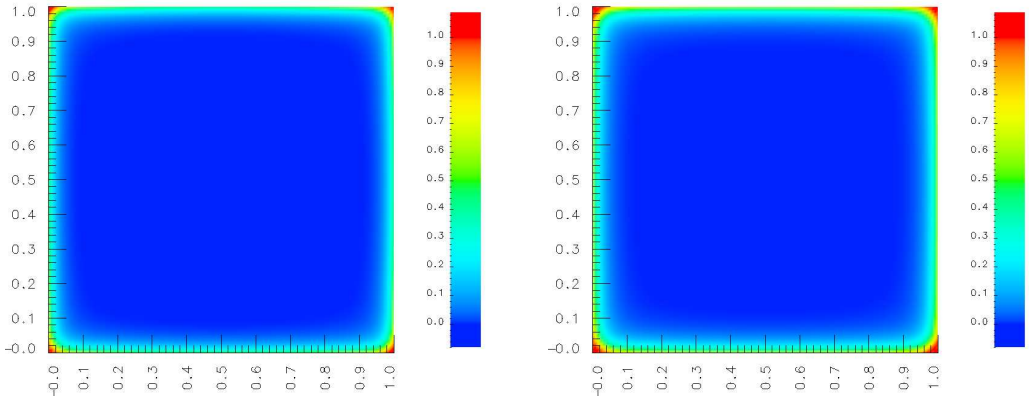

(e) $t = 0.20$

(f) $t = 0.25$

Figure 4.29: Evolution of Latent Heat with Smooth Interface: Model Problem 4 (Melting), $\Delta t = 0.01, 0 \leq t \leq 0.25$

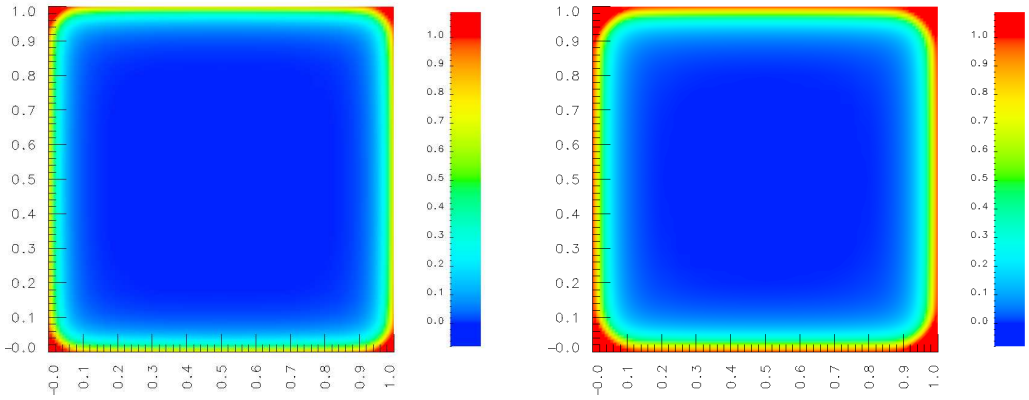

(a) $t = 0.35$ (b) $t = 0.50$

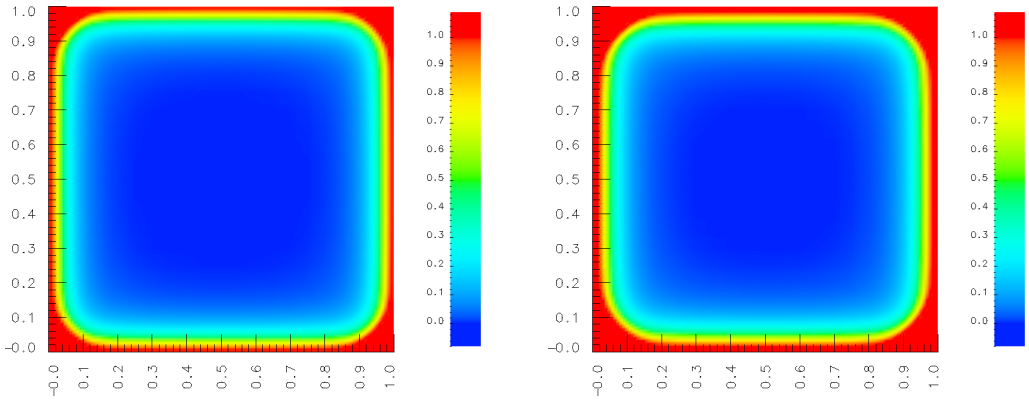

(c) $t = 0.65$ (d) $t = 0.80$

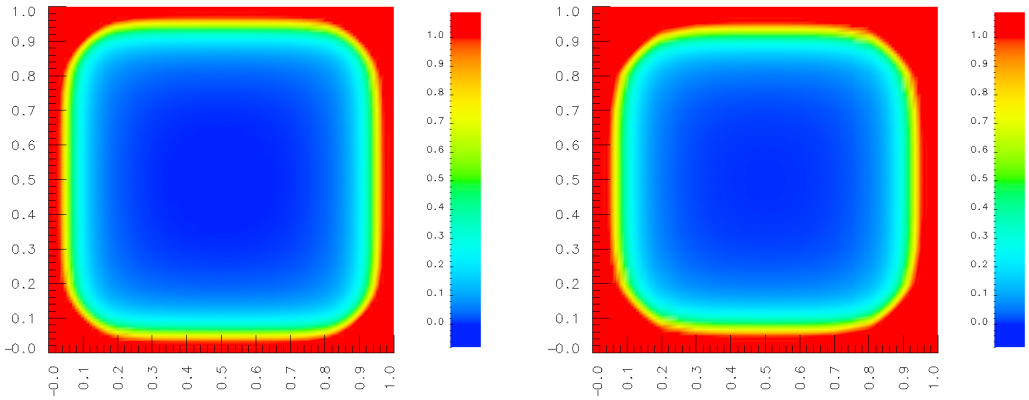

(e) $t = 1.00$ (f) $t = 1.25$

Figure 4.30: Evolution of Latent Heat (Smooth Interface): Model Problem 4, $\Delta t = 0.01$, $0.35 \leq t \leq 1.25$

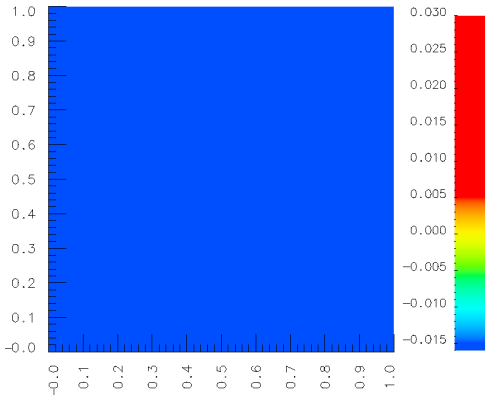

(a) Initial Condition

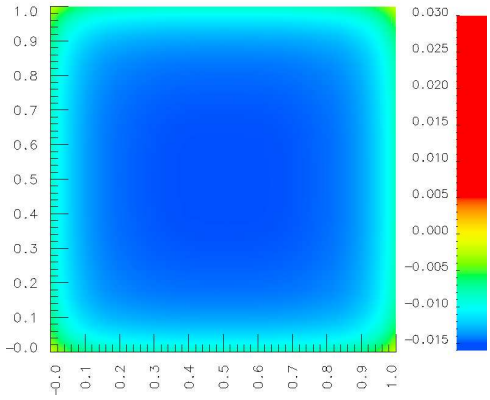

(b) $t = 0.01$

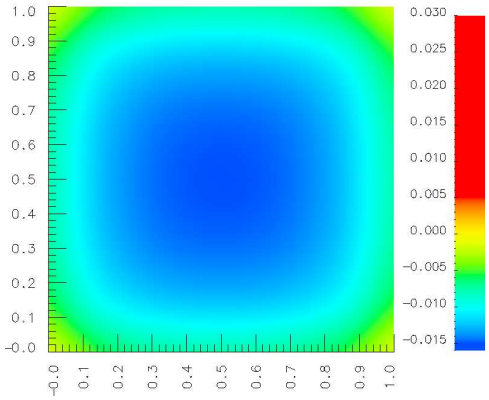

(c) $t = 0.02$

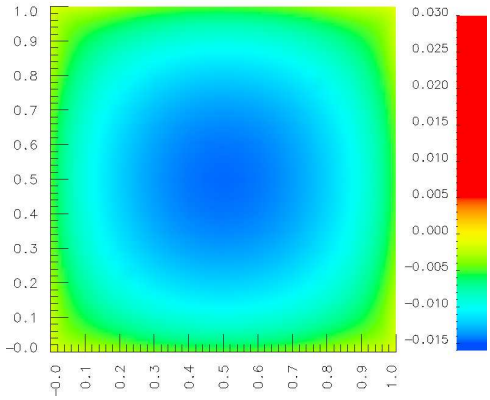

(d) $t = 0.03$

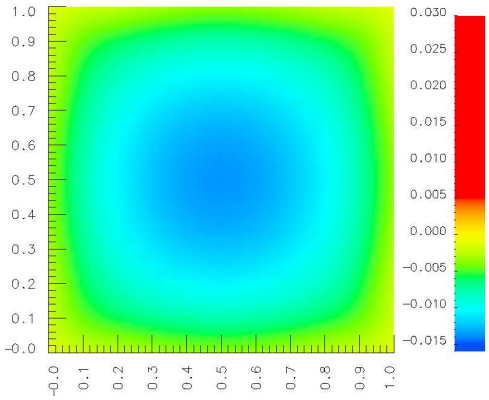

(e) $t = 0.04$

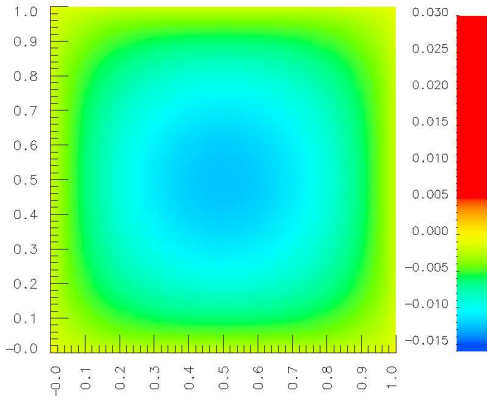

(f) $t = 0.05$

Figure 4.31: Evolution of Temperature (Smooth Interface): Model Problem 4, $\Delta t = 0.01$, $0 \leq t \leq 0.05$

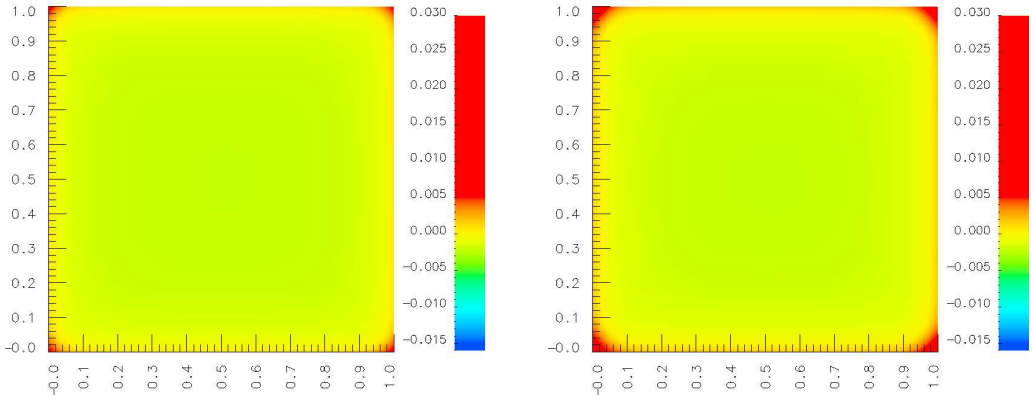

(a) $t = 0.35$ (b) $t = 0.50$

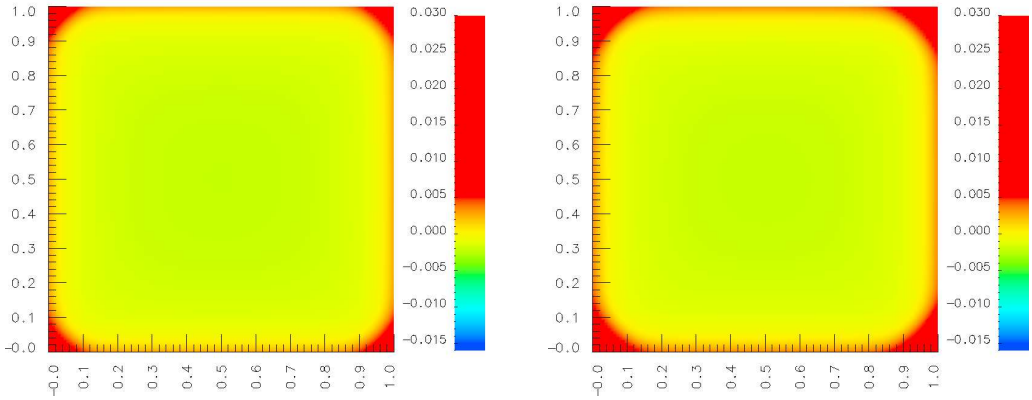

(c) $t = 0.65$ (d) $t = 0.80$

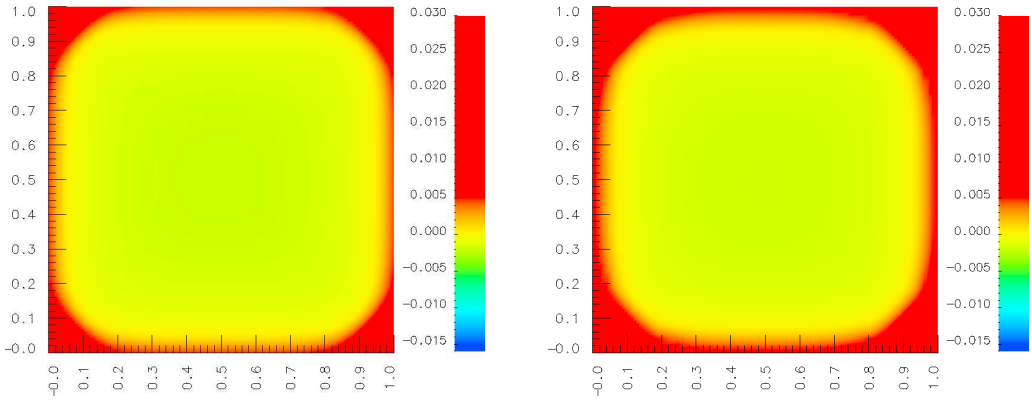

(e) $t = 1.00$ (f) $t = 1.25$

Figure 4.32: Evolution of Temperature (Smooth Interface): Model Problem 4, $\Delta t = 0.01$, $0.35 \leq t \leq 1.25$

Chapter 5

Summary and Conclusions

In this thesis numerical simulation of 1D and 2D liquid-solid or solid-liquid phase change phenomena have been presented using a smooth interface approach. Summary of this work and some conclusions drawn from this work are presented in this chapter.

The mathematical models of the phase-change physics are constructed in Lagrangian description with the assumptions of homogeneous and isotropic medium, no flow, and free boundaries. With these assumptions, the continuity and momentum equations are identically satisfied. Thus, only the first law of thermodynamics (energy equation), Fourier heat conduction law and the physics of phase change form the basis for deriving the mathematical model of phase change phenomena. The energy equation is expressed in terms of specific total energy and heat conduction. Fourier heat conduction law and the specific total energy, expressed in terms of internal energy and latent heat are substituted in the energy equation to derive a single non-linear PDE in temperature containing up to second order derivatives of the temperature with respect to spatial coordinates but only the first order derivatives of the temperature and latent heat with repect to time. Specific heat c_p, thermal

conductivity k and the latent heat of fusion L_f are all assumed to be functions of temperature. The physics of phase change is incorporated through a smooth interface between the two phases. We assume that the phase change occurs over a small temperature range $[T_s, T_l]$ referred to as the interface or transition region. In the transition region c_p, k and L_f are assumed to be continuous and differentiable functions of temperature. Outside the transition region, c_p and k have their respective values in the solid or liquid phases. Using $L_f = L_f(T)$, the time derivative of L_f in the energy equation is replaced by the derivative of the latent heat with respect to temperature and the time derivative of temperature. This yields the final form of the energy equation as a single non-linear diffusion equation in the temperature. Hence the location of the interface separating the two phases, its initiation from commencement of the evolution and the propagation of the interface location in the spatial domain during evolution are all intrinsic in this mathematical model. When using this mathematical model, no special methods are required for tracking the front. In sharp interface and phase field models, specification of the interface separating the two phases is essential as initial condition i.e. these models can not simulate initiation of the interface. In the present mathematical model, formation of the transition region from the commencement of the evolution and the two phases separated by the transition region upon further evolution is inherent in the mathematical model. It is well known that sharp interface model incorporating singular solutions are numerically most difficult without excessive upwinding. The phase field models on the other hand require a priori knowledge of a potential that is highly dependent on the application in addition to ICs defining the interface location at the commencement of the evolution. None of these restrictions, limitations and assumptions are present in the mathematical model considered in this work.

The numerical solutions of the non-linear PDE in temperature, spatial coordinates and

time (i.e. non-linear IVP) are obtained using space-time least squares finite element method in ***h,p,k*** framework [9, 11, 12, 22–25]. The PDE in temperature is recast as a system of first order PDEs using heat flux(es) and latent heat of fusion as dependent variables. This is done for the convenience of using C^0 p-version space-time local approximations for the space-time elements. Space-time least squares finite element processes yield unconditionally stable computations during the entire evolution regardless of the choice of h and p. The algebraic systems contain symmetric and positive definite coefficient matrices. The least squares functional I and its proximity to zero is an absolute measure of error in the computed evolution without the knowledge of a theoretical solution. This is an extremely important and intrinsic feature of the computational methodology used in the present work. The evolution described by the IVP is computed for an increment of time using a space-time strip (1D problems) and a space-time slab (2D problems) with time marching. We time march only when the least squares functional for the current increment of time is sufficiently close to zero. Thus, within the framework of computational infrastructure used here 'time accurate' evolutions are possible. The least squares functional values for all four model problems used in the present work are ensured to be sufficiently low during the entire evolution. This establishes good accuracy of the evolutions and their very close proximity to 'time-accurate' evolutions.

Numerical solutions are presented for four model problems. The first model problem is a 1D phase change problem with constant c_p and k (and same values in both phases) in which the initial condition at time zero defines the two phases separated by a sharp interface. This is done by defining the temperature field at time zero obtained by using the theoretical solution from the sharp interface model. This model problem is chosen primarily to show comparison of the of the smooth interface solutions with the sharp interface

theoretical solution and the numerical solutions from the phase-field model. Results presented in Section 4.3 of Chapter 4 show excellent agreement of the temperature evolution and interface location between the three approaches confirming that the proposed mathematical model and the computational infrastructure incorporates the sharp interface and phase field capabilities.

Model problem 2 is also a 1D phase-change problem in which at the commencement of the evolution we either have a solid phase or a liquid phase. The numerical studies demonstrate formation of the transition region, its propagation during evolution leading to two phases separated by the transition region. The studies demonstrate that the thin transition region does not diffuse during evolution (establishing lack of numerical dispersion in the computational method used in this work). c_p and k have their respective values in the solid and liquid phases. In the transition region, c_p, k and L_f are continuous and differentiable and are assumed to be a polynomial of third degree in temperature. Numerical studies are also presented to demonstrate that the width $[T_s, T_l]$ of the transition region does not influence the location of interface marked by the center of $[T_s, T_l]$. However, spatial discretization is influenced by this choice.

Model Problems 3 and 4 are two dimensional phase change problems demonstrating the capability of the smooth interface method to initiate the formation of the transition region and its evolution in two dimensional spatial domain without employing any special means. We remark that model problems 2, 3 and 4 require initiation of the transition region and hence, can not be simulated by the sharp interface and phase field models. Different values of c_p and k in liquid and solid phases present additional difficulties in sharp interface and phase-field models that are avoided the smooth interface approach. Even though all numerical studies only employ local approximations of class C^0 in space

and time using mathematical models that are a system of first order PDEs, the work by Surana et.al. [9, 12–15] has demonstrated the benefits of using a single PDE in temperature employing approximations in higher order spaces. This can be done easily without any difficulty.

In summary, the work presented in this thesis has the following important features: (i) Derivation of the mathematical model leading to a non-linear diffusion equation. (ii) Incorporating the phase-change physics through a transition region in which c_p, k, and L_f are continuous and differentiable, thereby avoiding singular nature of the evolution as in case of sharp interface. (iii) The model permits initiation of the interface i.e. transition region which can not be done in the other two methods used commonly for phase change problems. (iv) The model permits different c_p and k that may even be function of temperature in solid and liquid phases. (v) No special techniques are needed to track the solid-liquid or liquid-solid fronts as these features are intrinsic in the mathematical models. (vi) Computational infrastructure ensures unconditionally stable computations during the entire evolution and provides a computed measure of the solution accuracy which enables computations of time accurate evolutions. The extension of this work using mathematical models in Eulerian description permitting the study of phase change phenomena in flowing medium with constrained boundaries resulting in non-zero velocity and stress fields is currently being performed by the graduate students working in the computational mechanics program with Professor Surana.

Bibliography

[1] J. Stefan. *Ober einige Probleme der Theorie der Warmeleitung*. Sitzungsber. Akad. Wiss. Wien, Math.-Naturwiss. Kl., 1889.

[2] L.I. Rubinstein. *The Stefan Problem*. American Mathematical Society, Providence, twenty seventh edition, 1994.

[3] H.S. Carslaw and J.S. Jaeger. *Conduction of Heat in Solids*. Oxford University Press, New York, second edition, 1959.

[4] K. Krabbenhoft, L. Damkilde, and M. Nazem. An implicit mixed enthalpy-temperature method for phase-change problems. *Heat Mass Transfer*, 43:233–241, 2007.

[5] Sin Kim, Min Chan Kim, and Won-Gee Chun. A fixed grid finite control volume model for the phase change heat conduction problems with a single-point predictor-corrector algorithm. *Korean J. Chem. Eng.*, 18(1):40–45, 2001.

[6] M. Fabbri and V.R. Voller. The phase-field method in sharp-interface limit: A comparison between model potentials. *Journal of Computational Physics*, 130:256–265, 1997.

[7] John W. Cahn and John E. Hilliard. Free energy of a nonuniform system. i. interfacial free energy. *The Journal of Chemical Physics*, 28(2):1015–1031, 1958.

[8] Lev D. Landau, Evgenij Michailovič Lifšic, and Lev P. Pitaevskij. *Statistical Physics: Course of Theoretical Physics*. Pergamon Press plc, London, 1980.

[9] K.S. Surana. *Mathematics of computations and finite element method for initial value problems, ME 862 class notes*. University of Kansas, Department of Mechanical Engineering, Manuscript of textbook in preparation, 2010.

[10] T. Belytschko and T.J.R. Hughes. *Numerical solution of partial differential equations by finite element method*. North Holland, 1983.

[11] B.C. Bell and K.S. Surana. A space-time coupled p-version lsfef for unsteady fluid dynamics. *International Journal of Numerical Methods in Engineering*, 37:3545–3569, 1994.

[12] K.S. Surana, J.N. Reddy, and S. Allu. The k-version of finite element method for initial value problems: mathematical and computational framework. *International Journal of Computational Methods in Engineering Science and Mechanics*, 8:123–136, 2007.

[13] K.S. Surana, A. Ahmadi, and J.N. Reddy. k-version of finite element method for non-linear differential operators in bvp. *International Journal of Computational Engineering Science*, 5(1):133–207, 2004.

[14] K.S. Surana, A. Ahmadi, and J.N. Reddy. k-version of finite element method for self-adjoint operators in bvp. *International Journal of Computational Engineering Science*, 3(2):155–218, 2002.

[15] K.S. Surana, A. Ahmadi, and J.N. Reddy. k-version of finite element method for non-self-adjoint operators in bvp. *International Journal of Computational Engineering Science*, 4(4):737–812, 2003.

[16] Y. Ding, J.A. Gear, and K.N. Tran. A finite element modeling of thermal conductivity fabrics embedded with phase change material. *Heat Mass Transfer*, 43:233–241, 2007.

[17] M. Gelfand and S.V. Foming. *Calculus of Variations*. Dover, New York, 2000.

[18] S.G. Mikhlin. *Variational methods in mathematical physics*. Pergamon Press, New York, 1964.

[19] J.N. Reddy. *Functional analysis and variational methods in applied mechanics*. McGraw-Hill, New York, 1986.

[20] J.N. Reddy. *Energy principles and variational methods in applied mechanics*. John Wiley, New York, 2002.

[21] C. Johnson. *Numerical solution of partial differential equations by finite element method*. Cambridge University Press, 1987.

[22] K.S. Surana, S. Allu, J.N. Reddy, and P.W. Tenpas. Least squares finite element processes in *hpk* mathematical framework for non-linear conservation law. *International Journal of Numerical Methods in Fluids*, 57(10):1545–1568, 2008.

[23] D.L. Winterscheidt and K.S. Surana. p-version least squares finite element formulation for two dimensional incompressible fluid flow. *International Journal of Numerical Methods in Fluids*, 18:43–69, 1994.

[24] B.C. Bell and K.S. Surana. p-version least squares finite element formulation of two dimensional incompressible non-newtonian isothermal and non-isothermal fluid flow. *International Journal of Numerical Methods in Fluids*, 18:127–167, 1994.

[25] D.L. Winterscheidt and K.S. Surana. p-version least squares finite element formulation for burgers equation. *International Journal for Numerical Methods in Engineering*, 36:3629–3646, 1993.

[26] K.S. Surana. *Mathematics of computations and finite element method for boundary value problems, ME 861 class notes*. University of Kansas, Department of Mechanical Engineering, Manuscript of textbook in preparation, 2010.

[27] R. F. Almgren. Second-order phase field asymptotics for unequal conductivities. *SIAM J. Appl. Math.*, 59:2086–2107, 1999.